HR(A)TEN for Nano-electronic Materials Research

Moon Kim, R.M. Wallace, B.E. Gnade
Department of Electrical Engineering
University of Texas at Dallas

International Conference on Characterization and Metrology for ULSI Technology
March 15-18, 2005

2005 ULSI Metrology

✓ Session 7: Microscopy

- 10:00 AM STEM w/ Monochromator
- 10:30 AM HR(A)TEM for Materials Research
- 11:00 AM Aberration corrected SEM
- 11:30 AM Aberration corrected STEM

I have a theory!

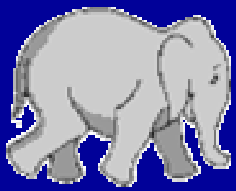

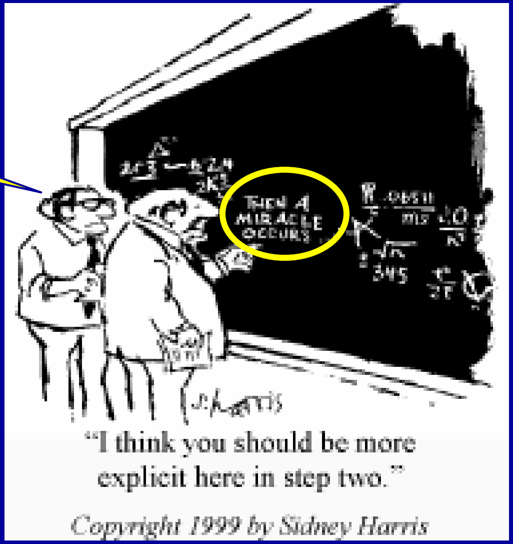

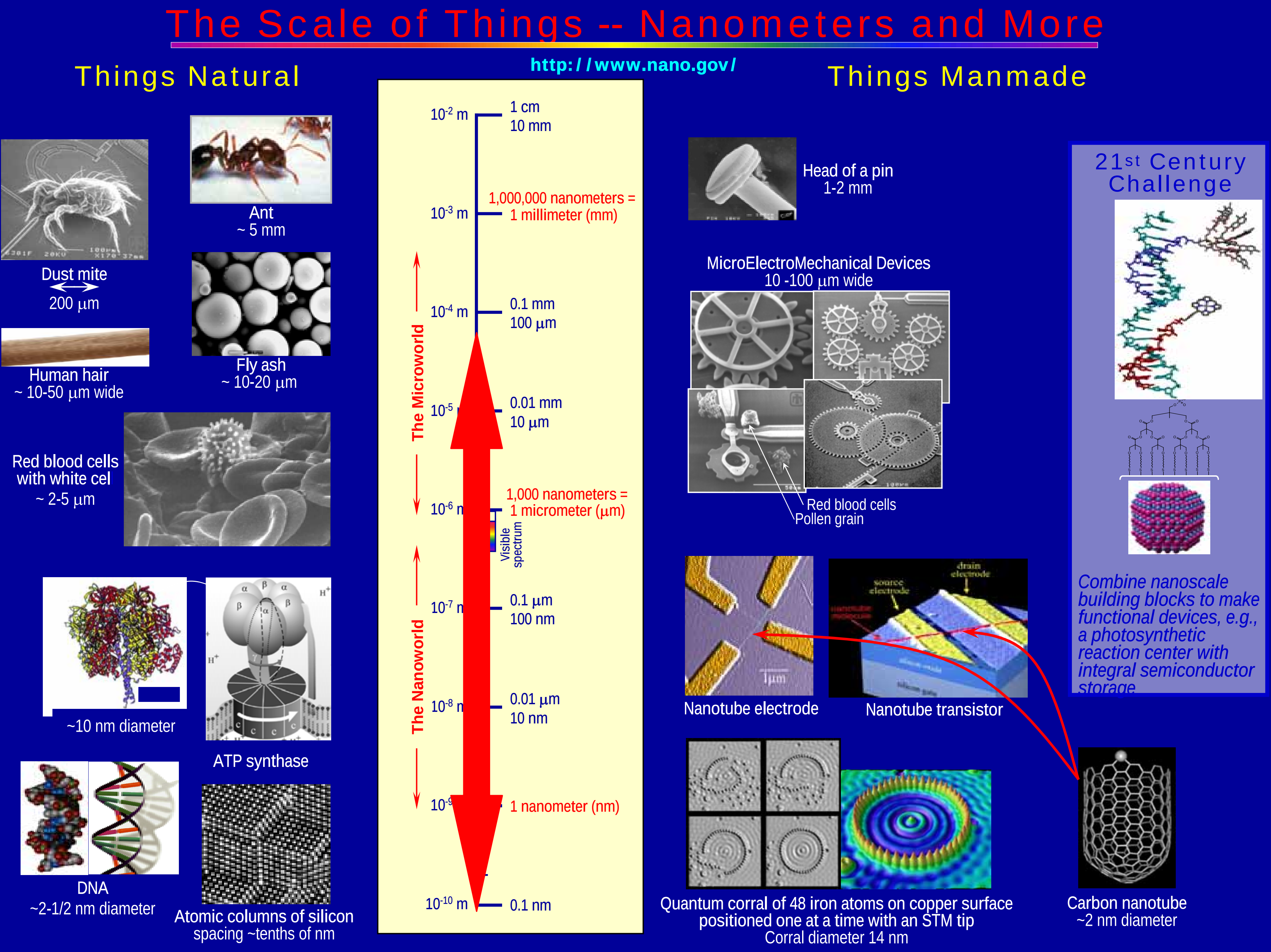

The Scale of Things -- Nanometers and More
http://www.nano.gov/
Things Natural
Things Manmade
Dust mite
200 µm
Ant
~ 5 mm
Human hair
~ 10-50 µm wide
Fly ash
~ 10-20 µm
Red blood cells
with white cel
~ 2-5 µm
~10 nm diameter
ATP synthase
DNA
~2-1/2 nm diameter
Atomic columns of silicon
spacing ~tenths of nm
10^-2 m
1 cm
10 mm
10^-3 m
1,000,000 nanometers =
1 millimeter (mm)
10^-4 m
0.1 mm
100 µm
The Microworld
10^-5 m
0.01 mm
10 µm
10^-6 m
1,000 nanometers =
1 micrometer (µm)
Visible spectrum
10^-7 m
0.1 µm
100 nm
The Nanoworld
10^-8 m
0.01 µm
10 nm
10^-9 m
1 nanometer (nm)
10^-10 m
0.1 nm
Head of a pin
1-2 mm
MicroElectroMechanical Devices
10 -100 µm wide
Red blood cells
Pollen grain
Nanotube electrode
Nanotube transistor
Quantum corral of 48 iron atoms on copper surface
positioned one at a time with an STM tip
Corral diameter 14 nm
Carbon nanotube
~2 nm diameter
21st Century Challenge
Combine nanoscale building blocks to make functional devices, e.g., a photosynthetic reaction center with integral semiconductor storage

Why HR(A)TEM?

- **High Resolution (Analytical) Transmission Electron Microscopy**
  - essential tool for investigators in nanoscale science and engineering
  - nanostructure and chemistry of materials down to an atomic scale
  - (3D information).
- **Image Resolution**
  - Atomic resolution structure imaging (coherent)
  - Atomic resolution Z-contrast STEM imaging (incoherent)
- **Atomic Column-by-Column Spectroscopy**
  - Probe size
  - Probe current
  - Detection sensitivity

$$\delta = 0.66 C_s^{1/4} \lambda^{3/4}$$

$$\delta = 0.43 C_s^{1/4} \lambda^{3/4}$$

$$d_{\min} = 1.1 \left(\frac{4 i_p}{\pi^2 \beta} + 0.37 \lambda^2 \right)^{3/8} C_s^{1/4}$$

$$i_p = \frac{\pi^2}{4} \beta d_{source}^2 \alpha^2$$

Element	*σ_k (cm^2 x 10^{-22})*	*σ_b (cm^2 x 10^{-22})*	*MMF (at. %)*	*MDN (atoms)*
B	111	38	0.2	2
N	19	12	1.0	9
F	4.8	1.2	1.1	10
Ca	87	21	0.2	3
S	325	60	0.08	1

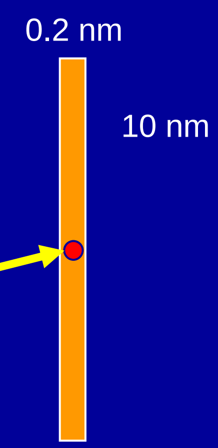

Minimum Mass Fraction (MMF) and Minimum Detectable Number of Atoms (MDN) within a 10-nm thick carbon matrix. MDN values are for an incident-beam diameter of 0.2 nm.

"Electron Energy Loss Spectroscopy in the Electron Microscope," R.F. Egerton, 1986.

Advanced EM Facility

✪ Instrumentation

- ❖ Dual column FIB (FEI Nova NanoLab 200) with Zyvex nanomanipulator
- ❖ High resolution Imaging FEG TEM (JEOL 2100F)
- ❖ High resolution Analytical FEG TEM/STEM with remote microscopy
- ❖ Comprehensive Sample Preparation Lab.
- ❖ Computing/Visualization Lab.
- ❖ Cryo, STM-TEM nanofactory, 3D tomography

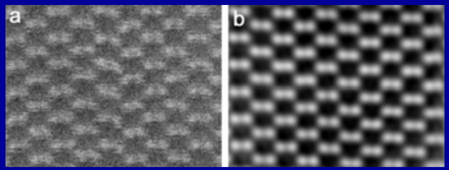

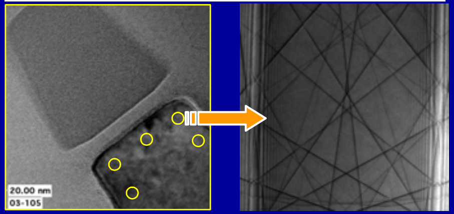

New NSM Research Facility

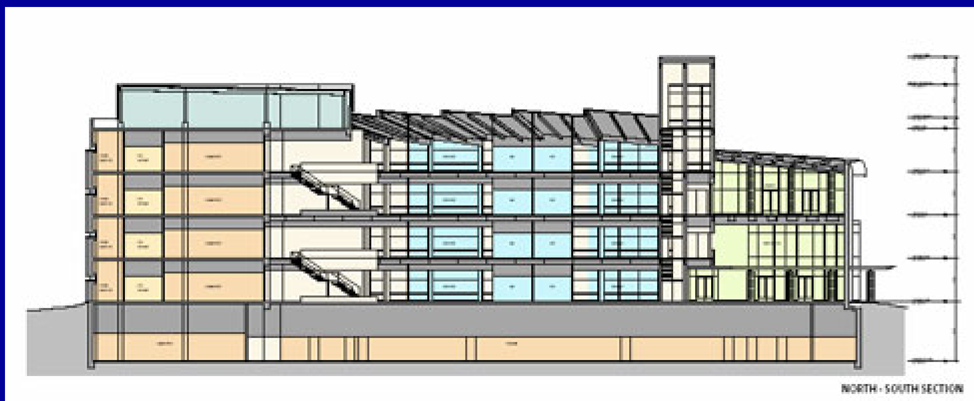

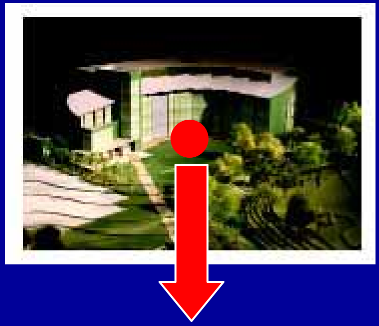

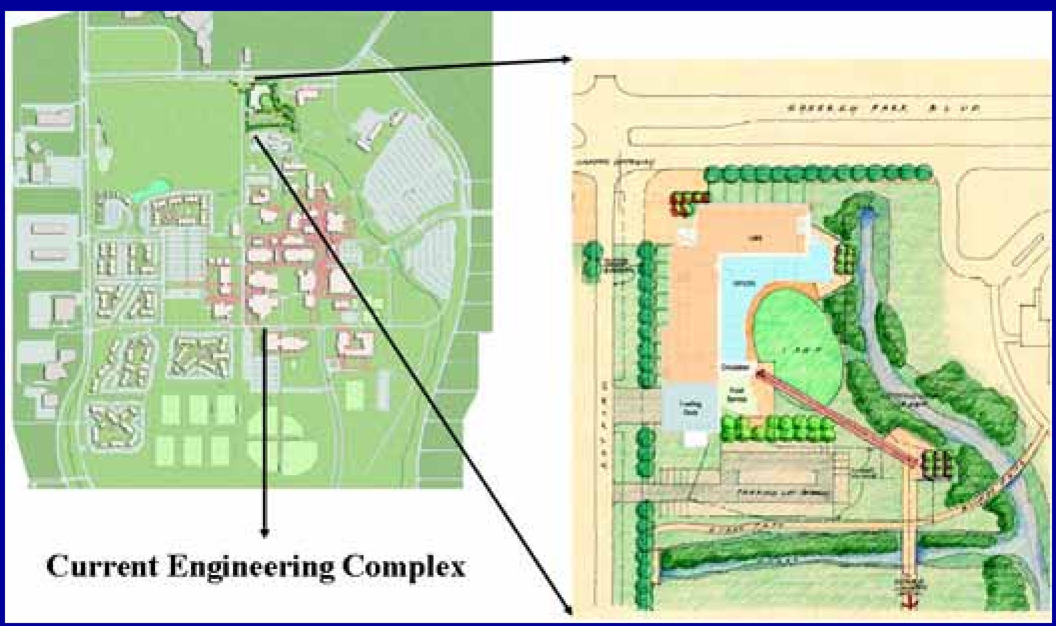

- ✓ Dedicated EM facility
  - – Vibration
  - – EM field
  - – Temperature
  - – Air flow & pressure
  - – Acoustic

Under the Microscope?

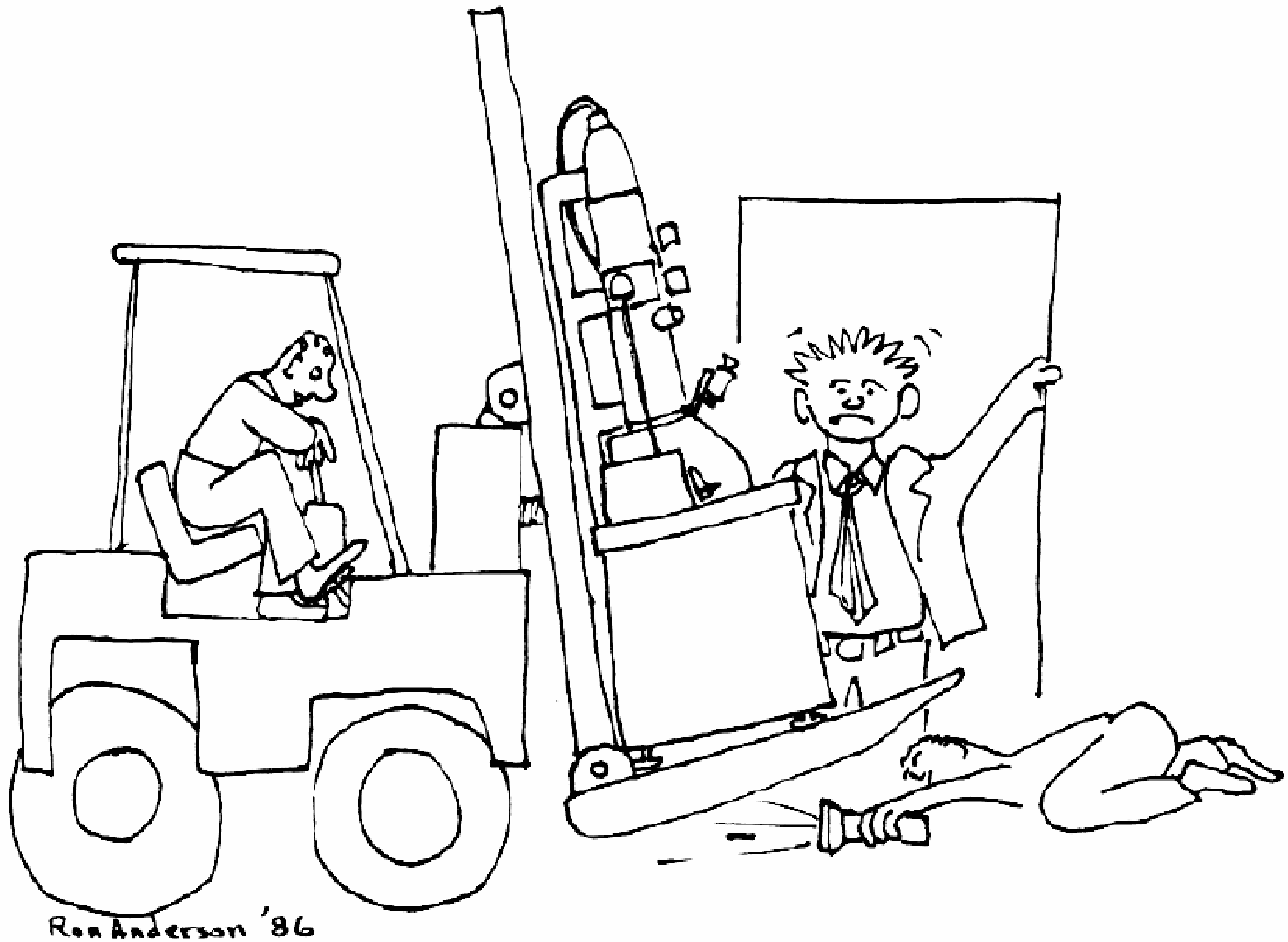

That's not what I had in mind when I said examine the specimen under the microscope.

TEM Techniques – Now and Then

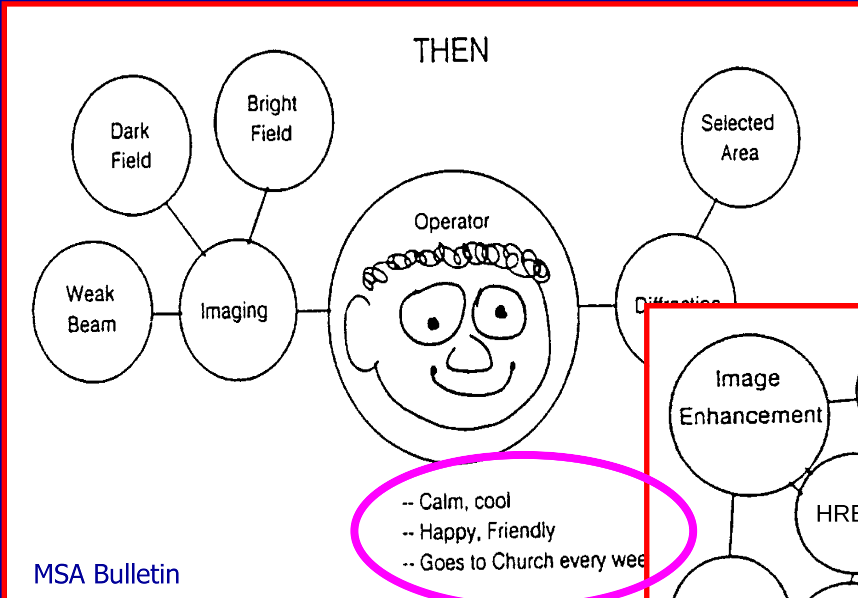

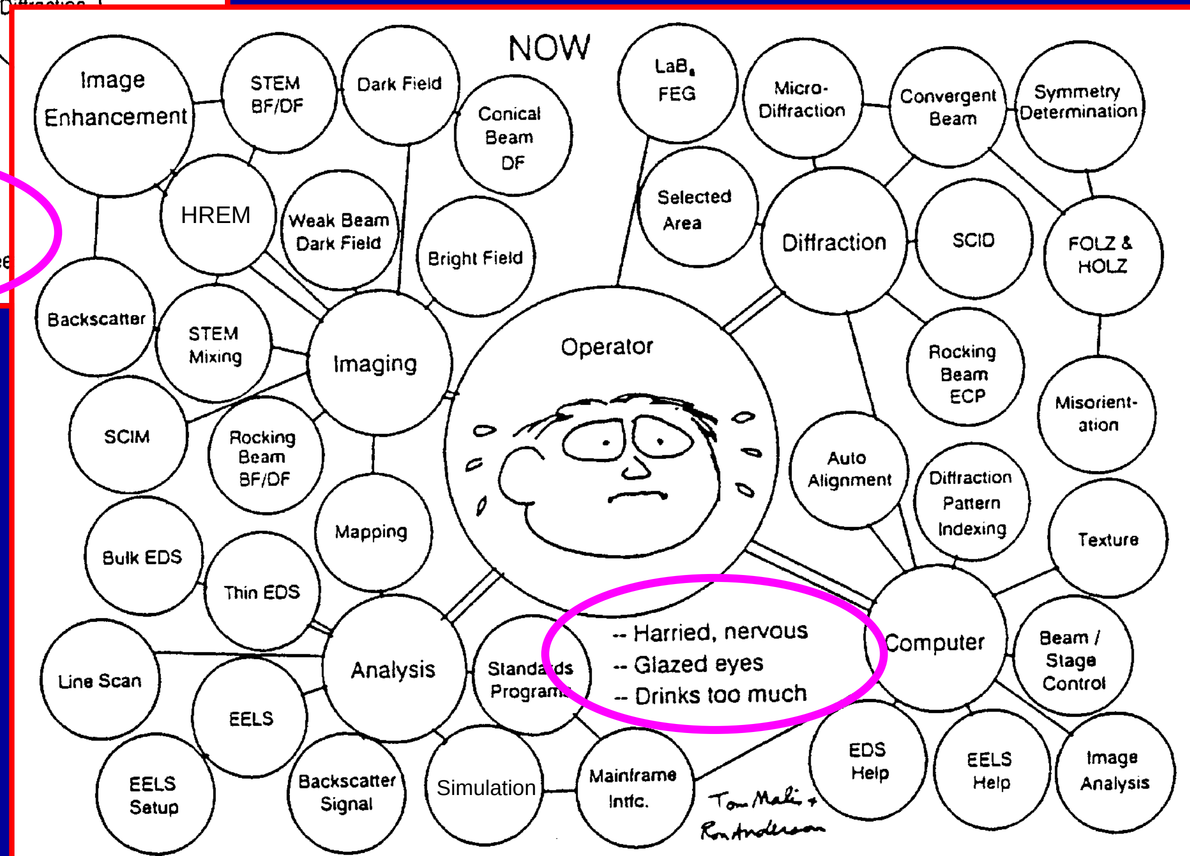

- Monochromator
- Cs corrector - STEM
- Cs corrector - HREM

HR(A)TEM: Application to Nano-X Materials

- ✓ Thermal stability of high-k gate dielectric films
  - Current SiO_2 gate oxide
  - ALCVD ZrO_2-based
  - $HfSiO_4$-based
  - $HfSi_xO_yN_z$-based
- Ultra low-k dielectric films
  - Nanoscale structural damage by plasma ash/etch
- Ni-silicides
  - Thin film morphology and phase identification
- Nanoscale lattice strain in Si CMOS Devices
  - New method of measuring local nanoscale strains

Current SiO_2 gate dielectric

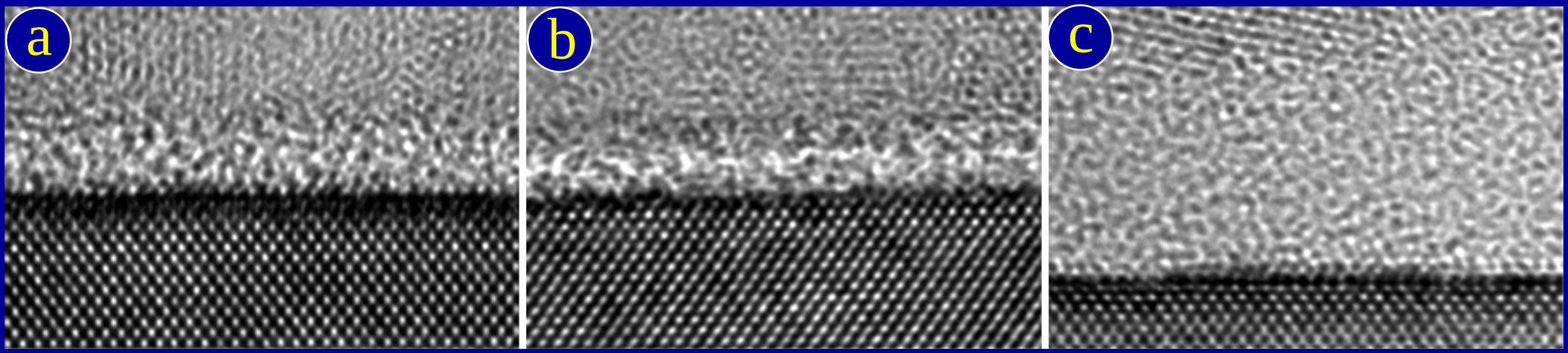

- Cross-sectional high resolution TEM images of poly-Si/SiO_2/Si interfaces: (a) as-deposited and (b) after rapid thermal annealing (RTA) at 1050ºC for 60 sec. (c) Thick gate oxide after RTA at 1050ºC for 60 sec. The observed amorphous SiO_2 gate oxides are thermally stable, as expected at this temperature.

"Only problem with SiO_2 … low-k."

High Resolution EELS for Si-O

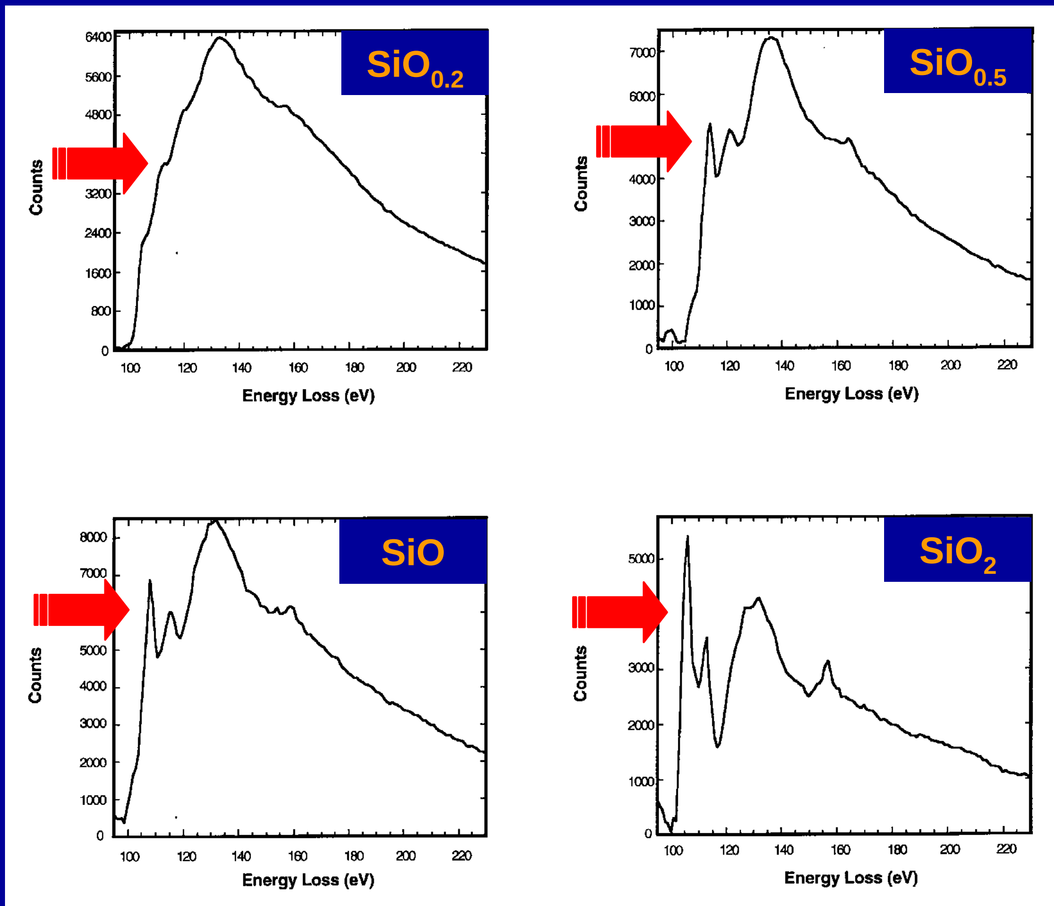

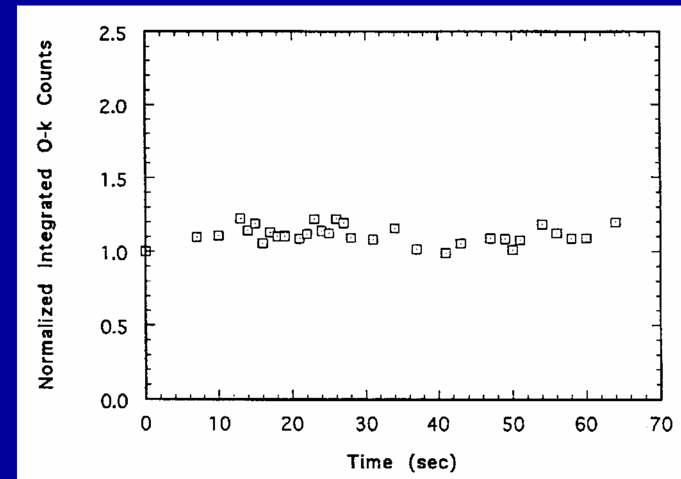

- Time-resolved O-K edge EELS plot for sub-stoichiometric silicon oxide thin films. ["Quantitative Analysis of Silicon Oxide using EELS," M.J. Kim, *Proc. 52nd MSA*, 986-987 (1994)].

- Si-L edge of various silicon oxygen compounds. Marked differences exist in the near edge fine structure, showing changes in bonding from covalent bonding in Si to nearly complete ionic bonding in SiO_2. The onset of the Si-L edge from SiO_x is also reduced relative to SiO_2. [Catalano, Kim, Carpenter, Das Chowdhury and Wong, *J. Mater. Res*. **8**, 2893-2901 (1993)].

Crystalline vs. Amorphous Gate Dielectric

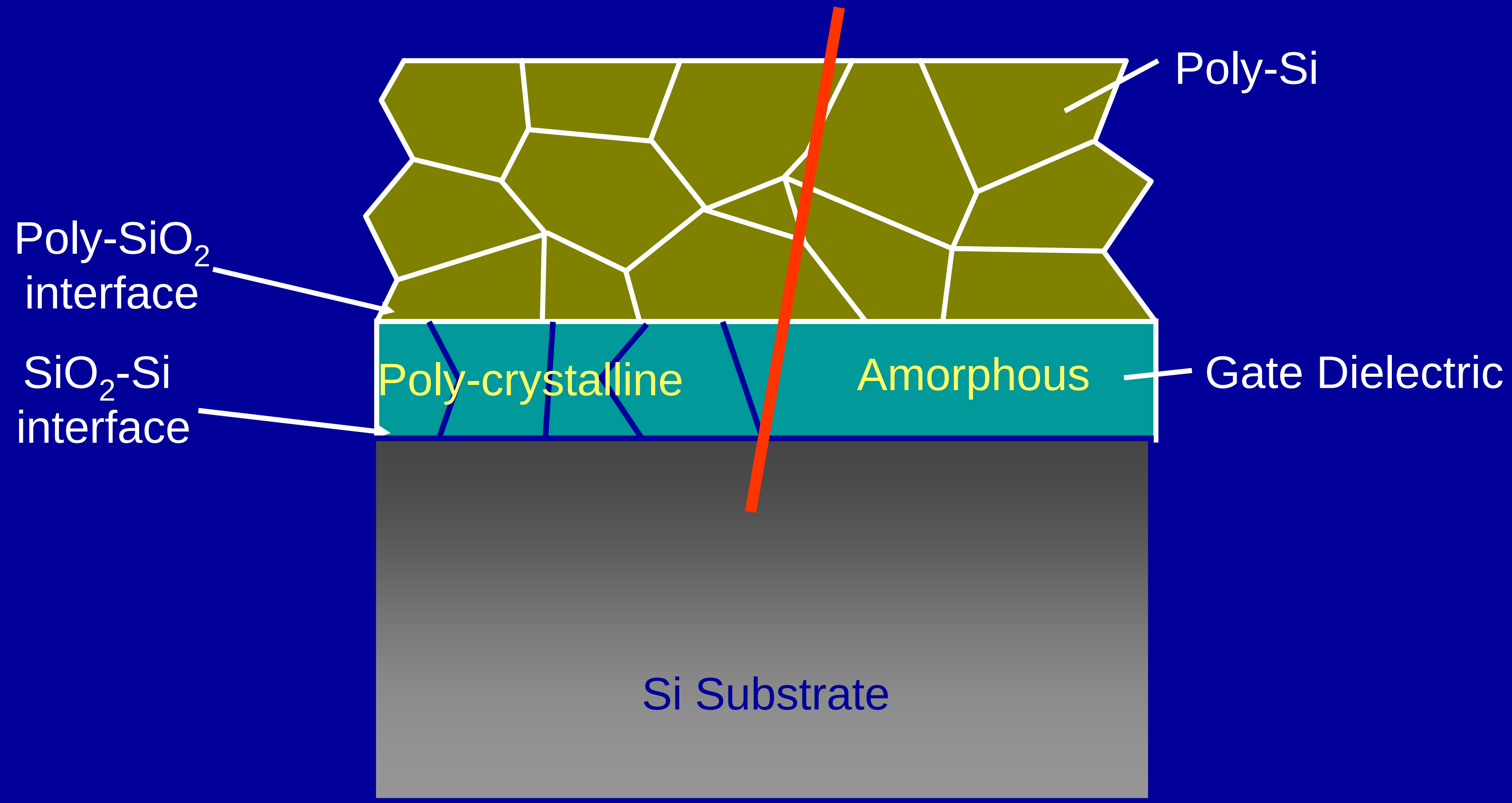

Amorphous Advantages

- Robust, thermal SiO_2 the benchmark
- Avoids orientation/grain size dependence of polarizibility
- Avoids enhanced leakage or diffusion through grain boundaries
- New single crystal dielectrics require Epitaxial approach

ZrO_2-based: as-deposited

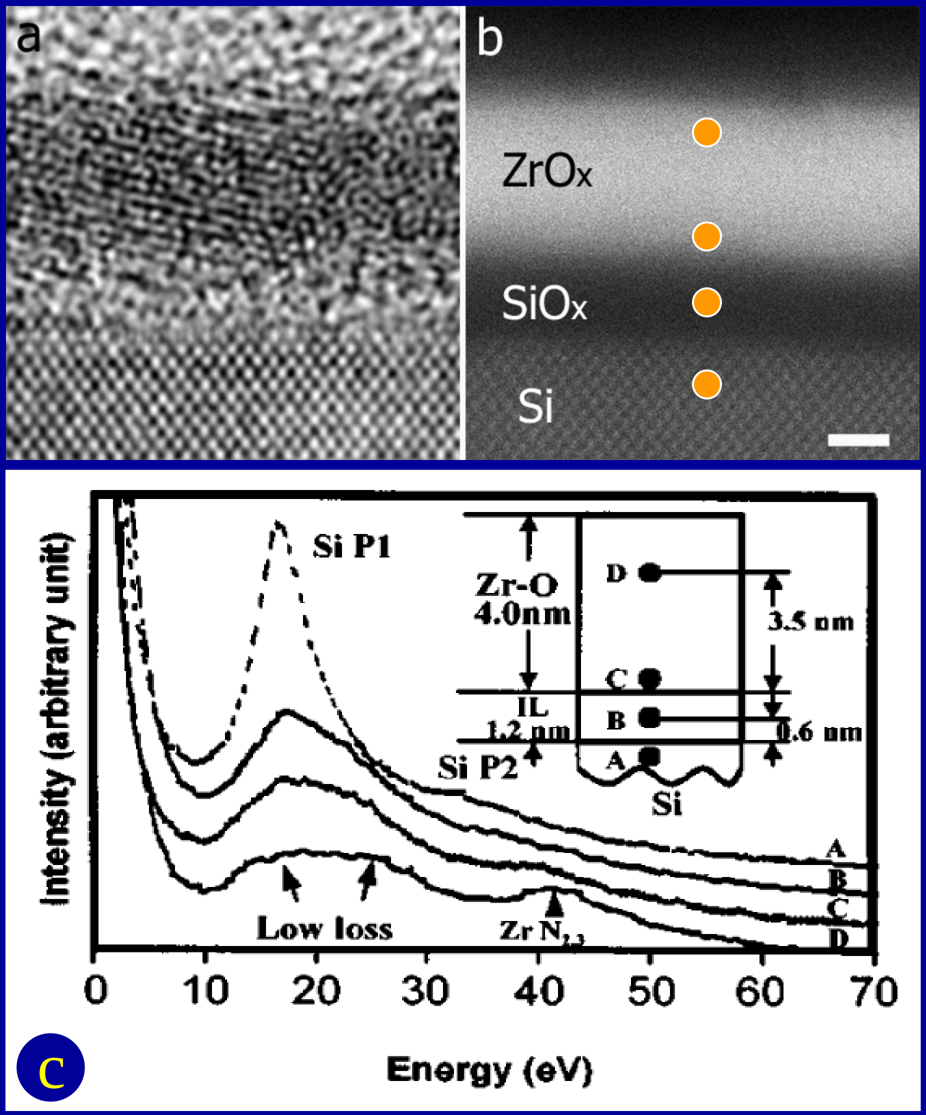

(a) High Resolution TEM, (b) high resolution annular dark field (ADF) images of as-deposited ALCVD Zr-O/SiO_x/Si stack. (c) A series of nanoprobe high spatial resolution electron energy loss spectra (EELS) of as-deposited Zr-O/SiO_x/Si stack shown in (a). The spectra are displaced vertically for easy shape comparison. Note nanocrystalline nature of the as-deposited film.

[Dey, Wang, Tang, Kim, Carpenter, Werkhoven and Shero, *J. Appl. Phys*. **93**, 4144 (2003)]

ZrO_2-based: as-deposited

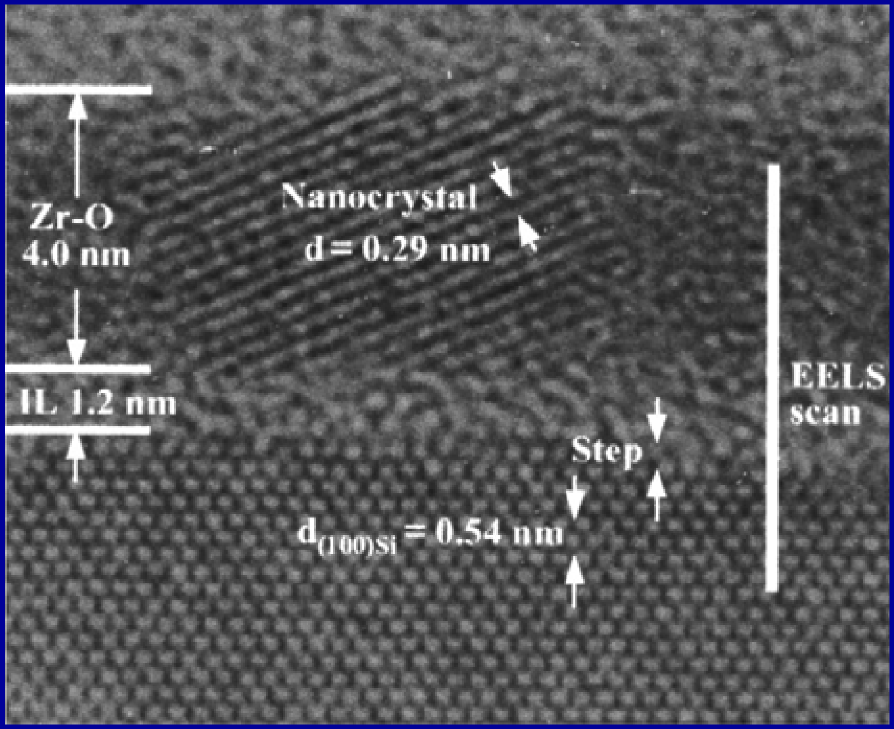

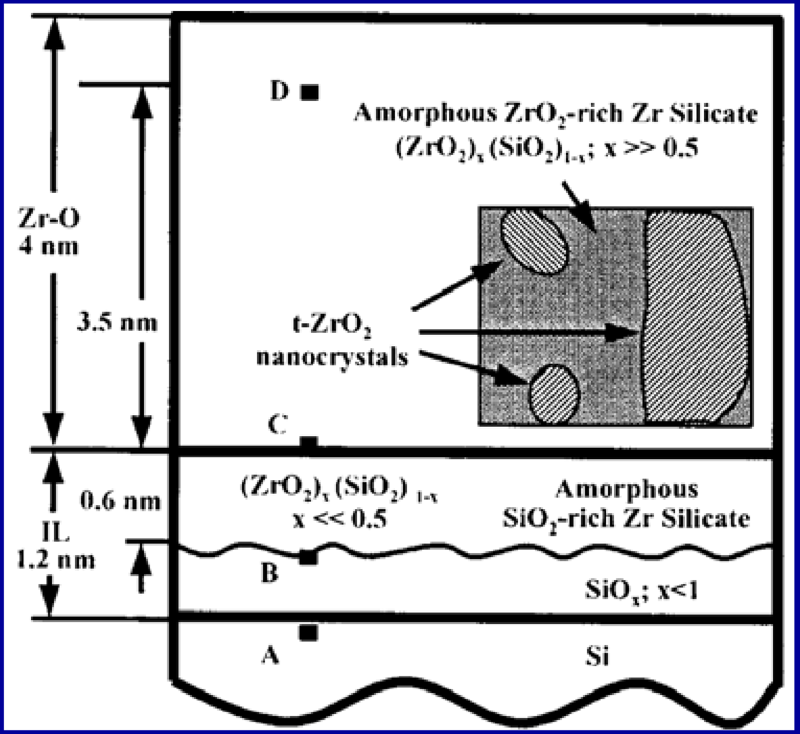

- Nanostructure and nanochemistry of the as-deposited ALCVD Zr-O/SiO_x/Si stack. The Zr-O layer is a compositionally graded ZrO_2-rich Zr silicate glass with nanocrystalline precipitates, and the interlayer (IL) is an amorphous bilayer of SiO_x and compositionally graded SiO_2-rich Zr silicate.

ZrO_2-based: annealed

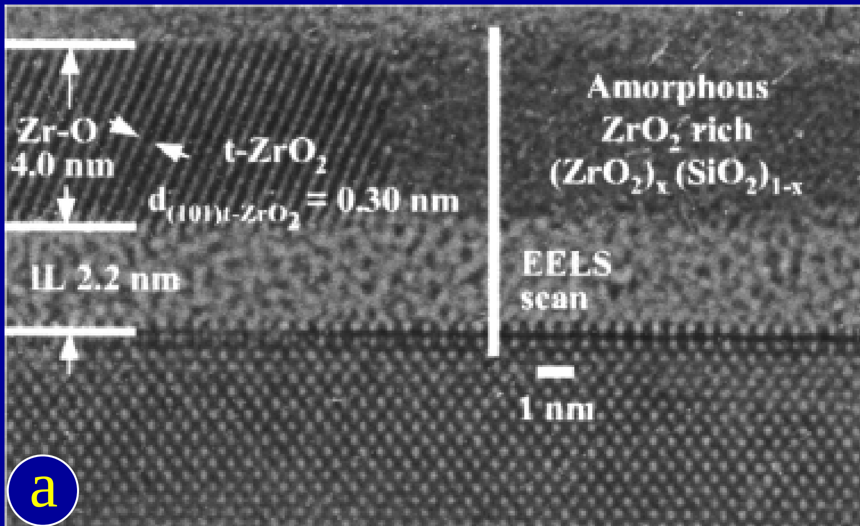

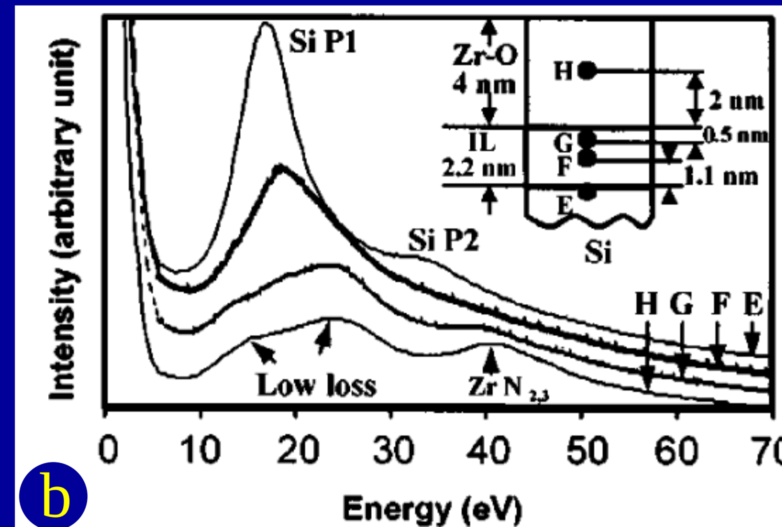

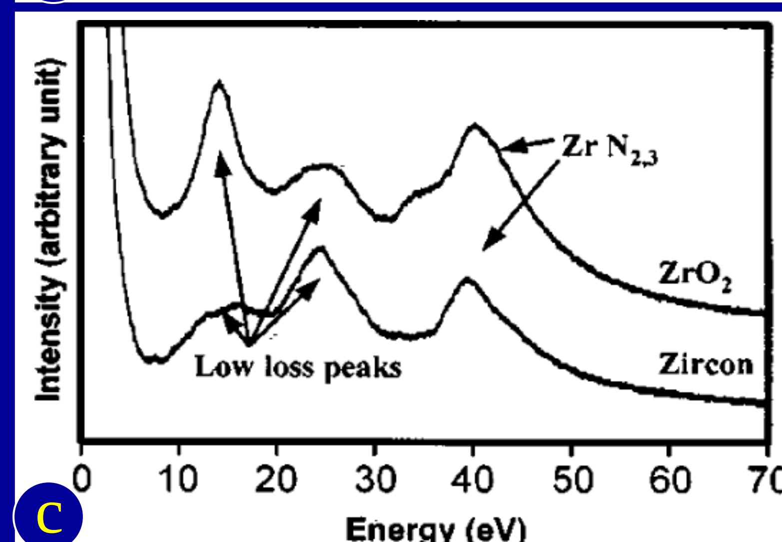

(a) HRTEM image of annealed Zr-O/SiO_x/Si stack. (b) A series of nanoprobe EELS spectra of annealed Zr-O/SiO_x/Si stack shown in (a). (c) EELS spectra of standard single crystalline (stoichiometric) specimens. The spectra are displaced vertically for easy shape comparison.

$ZrO_2/SiO_2/Si$

- Wafer Bonded → single crystal ZrO_2 on SiO_2/Si(100)

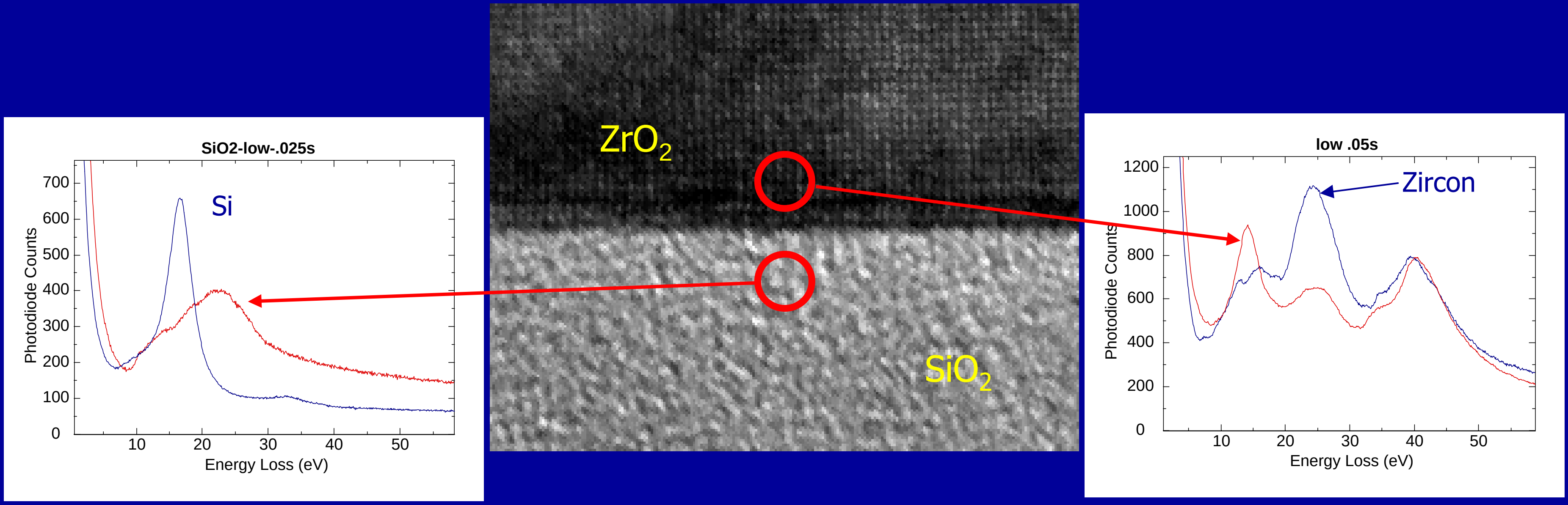

- HREM image of the bonded ZrO_2/SiO_2 interface (center), together with high spatial resolution EELS spectra from the amorphous (left) and crystalline (right) regions adjacent to the interface. The interface is sharp structurally and chemically down to atomic scale. [Kim and Carpenter, *J. Electronic Mater*. **32**, 849-854 (2003)]

ZrO_2-based: annealed

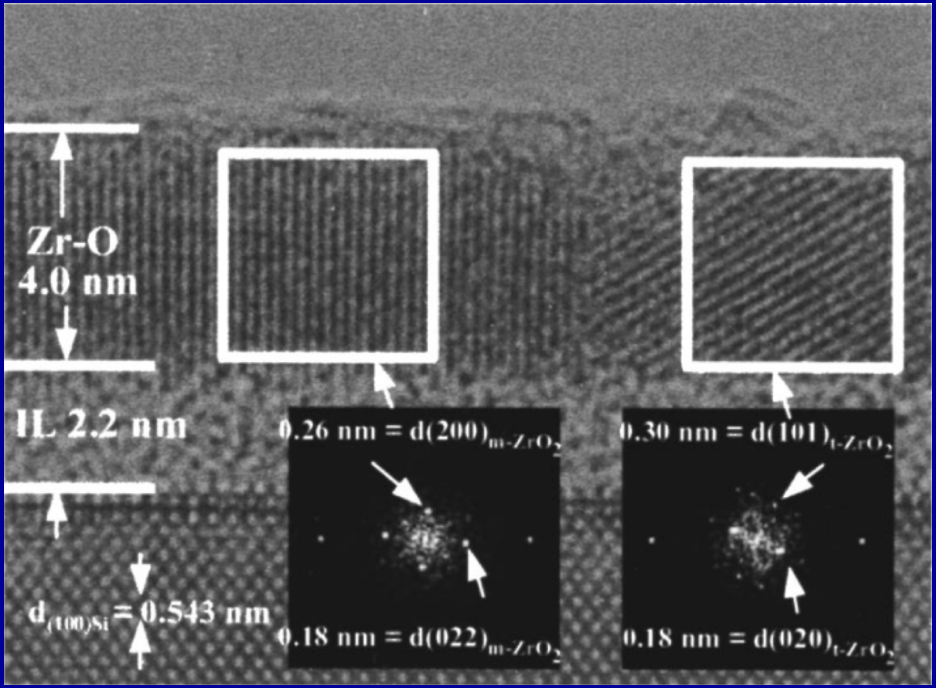

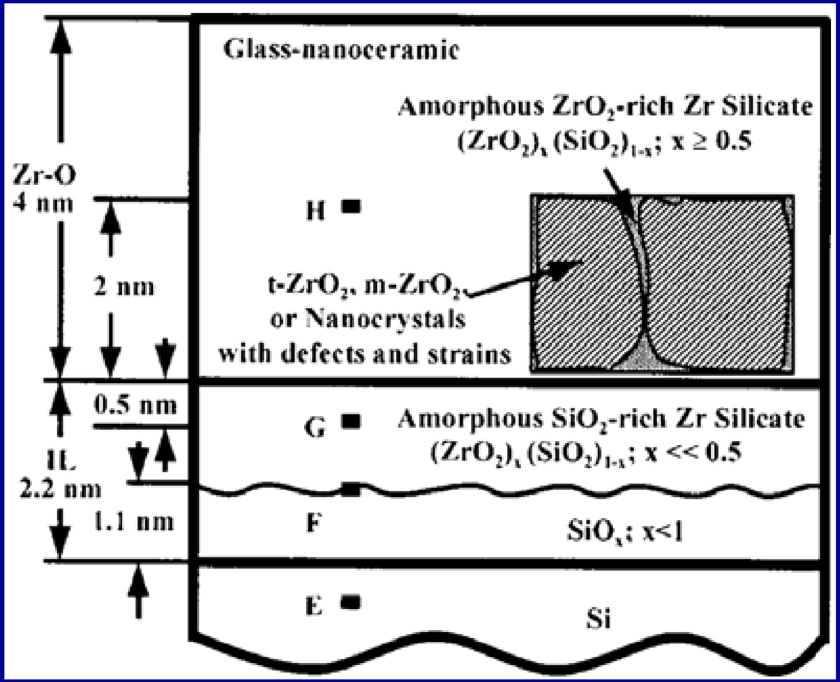

- Nanostructure and nanochemistry of the annealed ALCVD Zr-O/SiO_x/Si stack. The Zr-O layer is a heterogeneous glass nanoceramic. The thick interlayer (IL) is partitioned into an upper SiO_2-rich Zr silicate and the lower SiO_x. The latter is substoichiometric and the average oxidation state increased from $Si^{0.86+}$ in $SiO_{0.43}$ (as-deposited) to $Si^{1.32+}$ in $SiO_{0.66}$ (annealed). This high oxygen deficiency in SiO_x is indicative of the low mobility of oxidizing specie in the Zr-O layer.

$HfSi_xO_y$: as-deposited

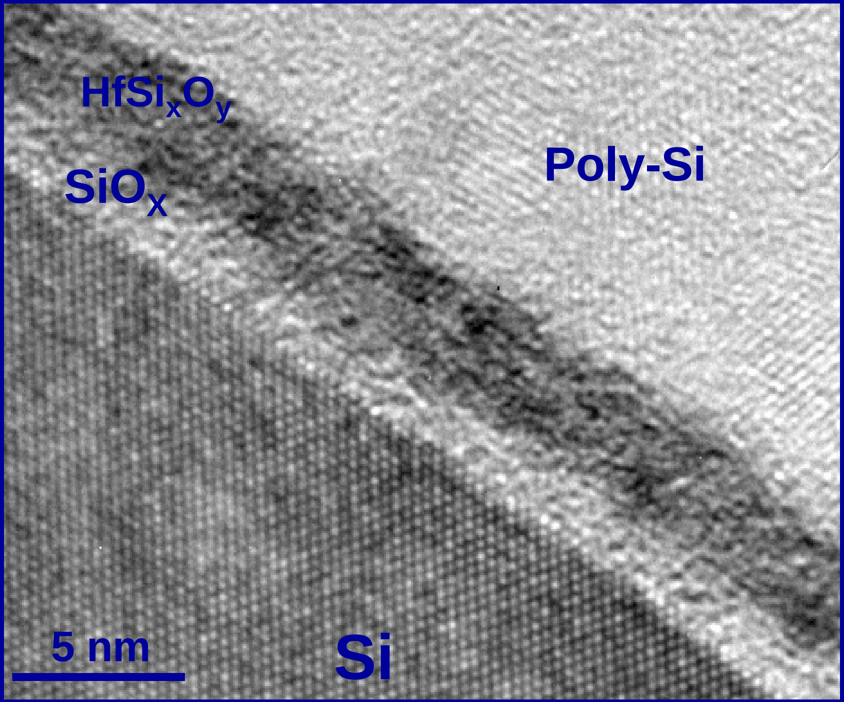

- As-deposited Hf-silicate film is amorphous.
- Silicate composition:
  - $(HfO_2)_{0.48}(SiO_2)_{0.52}$
- The ~5 nm dielectric film consists of:
  - ~1 nm SiO_x and ~4 nm $HfSi_xO_y$

[Quevedo-Lopez, Cl-Bouanani, Kim, Gnade, Wallace, Visokay, LiFatou, Bevan and Colombo, *Appl. Phys. Lett*. **81**, 1074 (2002)]

B-doped $HfSi_xO_y$: 1050°C / 60s RTA

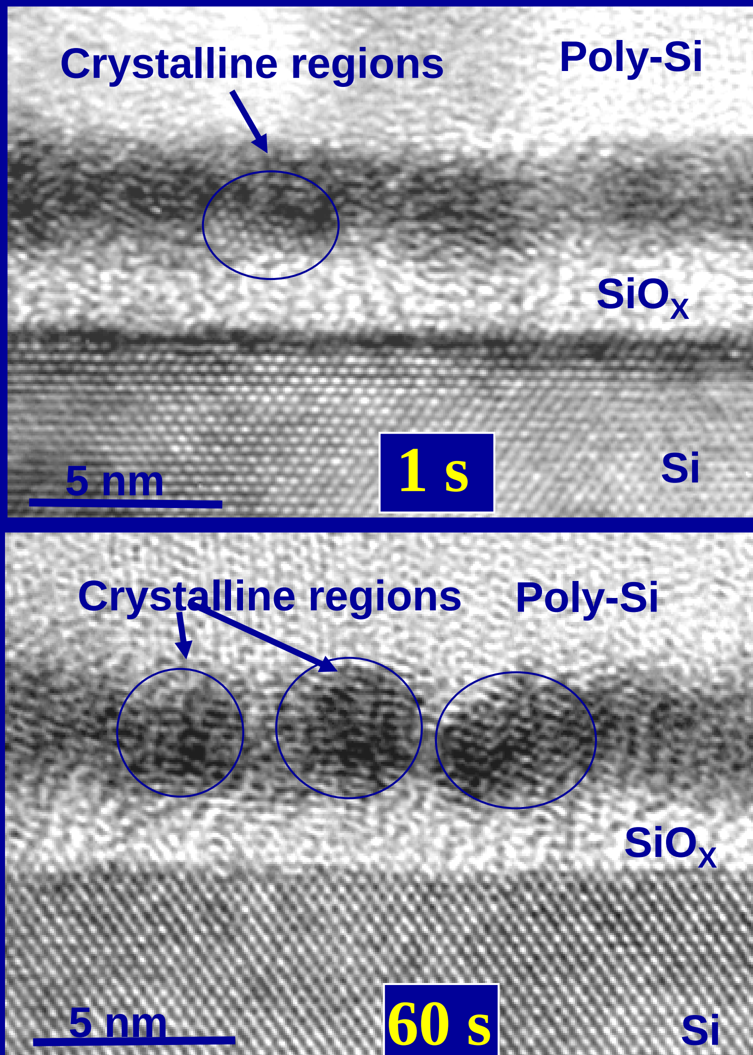

- Nanocrystalline regions observed after 1s RTA anneal
- Crystalline regions appears to be tetragonal HfO_2
- Consistent with Hf composition
  – $(HfO_2)_{0.48}(SiO_2)_{0.52}$
- Longer annealing times
  → more crystallization
  → higher B penetration

[Quevedo-Lopez, Cl-Bouanani, Kim, Gnade, Wallace, Visokay, LiFatou, Bevan and Colombo, *Appl. Phys. Lett.* **81**, 1074 (2002)]

P- and As-doped $HfSi_xO_y$: 1050°C / 60s RTA

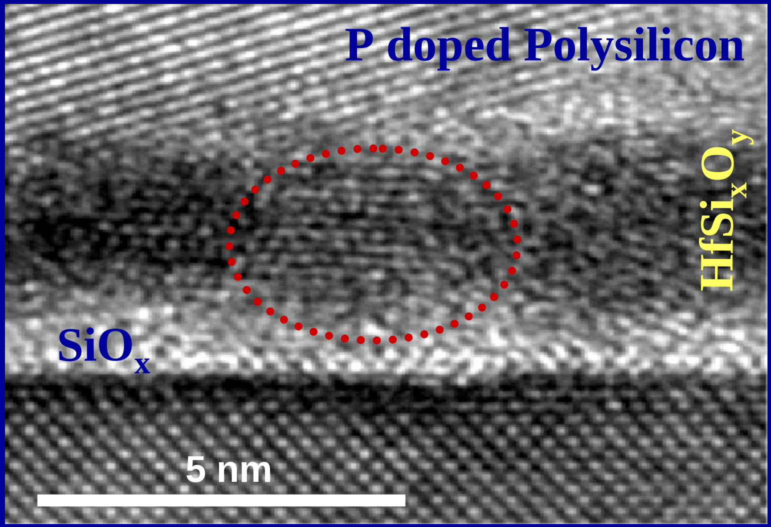

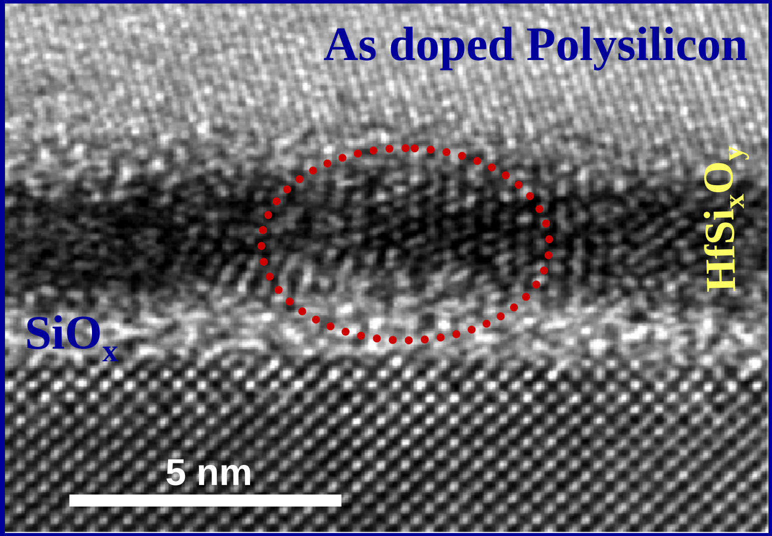

- Both films show crystallization after annealing, consistent with the B doped films results
- No effect of the dopant on crystallization the $HfSi_xO_y$ films
- No evident growth of the SiO_x interfacial layer after annealing

[Quevedo-Lopez, Cl-Bouanani, Kim, Gnade, Wallace, Visokay, LiFatou, Bevan and Colombo, *Appl. Phys. Lett*. **81**, 1609 (2002)]

Nitrogen Incorporation in $HfSi_xO_y$

- Brown found that k ↑ as N ↑ in the SiO_2 film.
  - → However, a major drawback in increasing the N content: decreases the band gap, decreasing the barrier height for electron and hole tunneling.*
- Si-O-N film acts like the diffusion barrier to impurities (such as B, P and As) from the poly-Si gate. Lesser diffusion in $HfSi_xO_yN_z$ as compared to $HfSi_xO_y$ has been observed.
- Better thermal stability.
- Only small amount of N incorporation is needed.

[* D. M. Brown, P. V. Gray, F. K. Heumann, H. R. Philipp, and E. A. Taft, *J. Electrochem. Soc.* **115**, 311 (1968)]

$HfSi_xO_yN_z$: with ~5-6 at.% Hf and ~18 at.% N

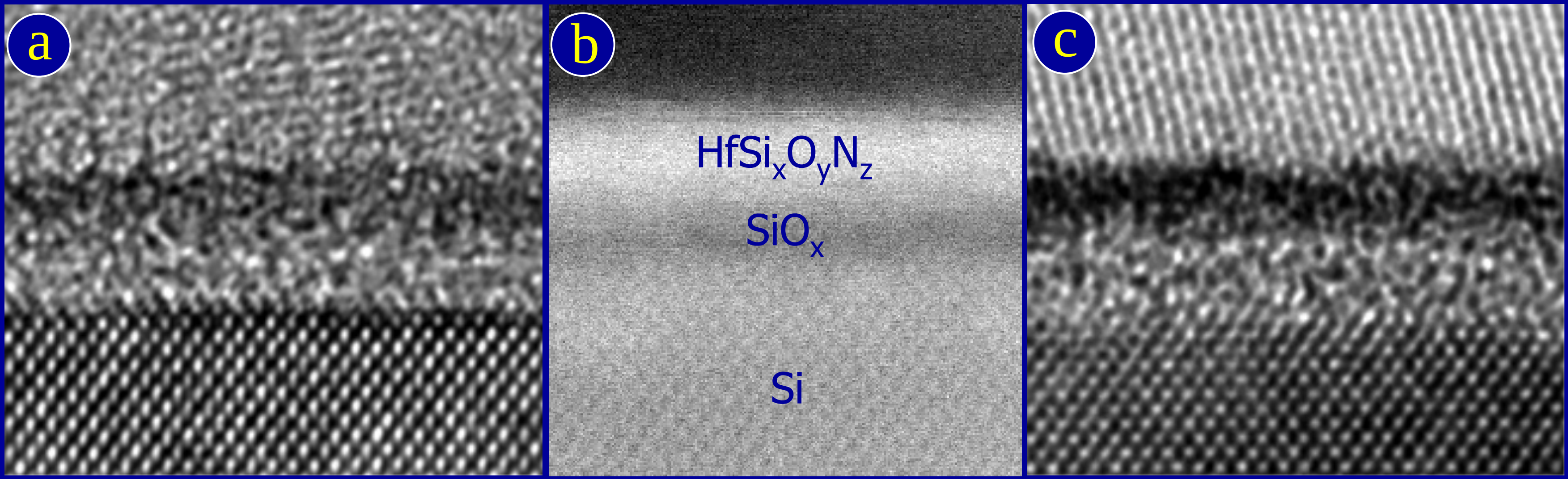

- Cross-sectional TEM images of the poly-Si capped $HfSi_xO_yN_z$ thin films on Si(100): (a) as-deposited (HREM), (b) as-deposited (ADF STEM), and (c) 60 sec RTA at 1050ºC. The total physical thickness is ~ 2.5 nm with an intentional interfacial (SiO_x) layer of ~ 1.1 nm.
- No detectible crystalline regions are observed.

[Quevedo-Lopez, Cl-Bouanani, Kim, Gnade, Wallace, Visokay, LiFatou, Chambers and Colombo, *Appl. Phys. Lett*. **82**, 4669 (2003)]

$HfSi_xO_yN_z$: with higher Hf content

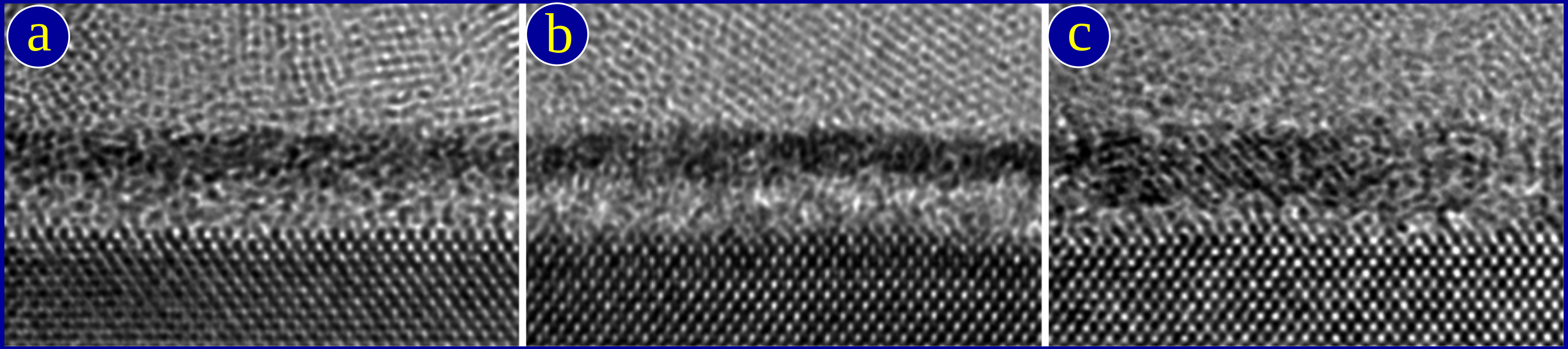

- Cross-sectional HRTEM images of the poly-Si capped $HfSi_xO_yN_z$ thin films with higher Hf content on Si(100), compared with the previous ones: (a) as-deposited, (b) 1 sec and (c) 60 sec RTA at 1050ºC.
- $HfSi_xO_yN_z$ films with high Hf content are thermally stable after a "spike" anneal for 1 sec, but crystallization was observed after 60 sec.
- A slight thickening of the $HfSi_xO_yN_z$ layer is also noticed, indicating a volume change associated with the crystallization as well as inter-diffusion of Hf and Si upon extended annealing.

$HfSi_xO_yN_z$: with thicker $HfSi_xO_yN_z$ layer

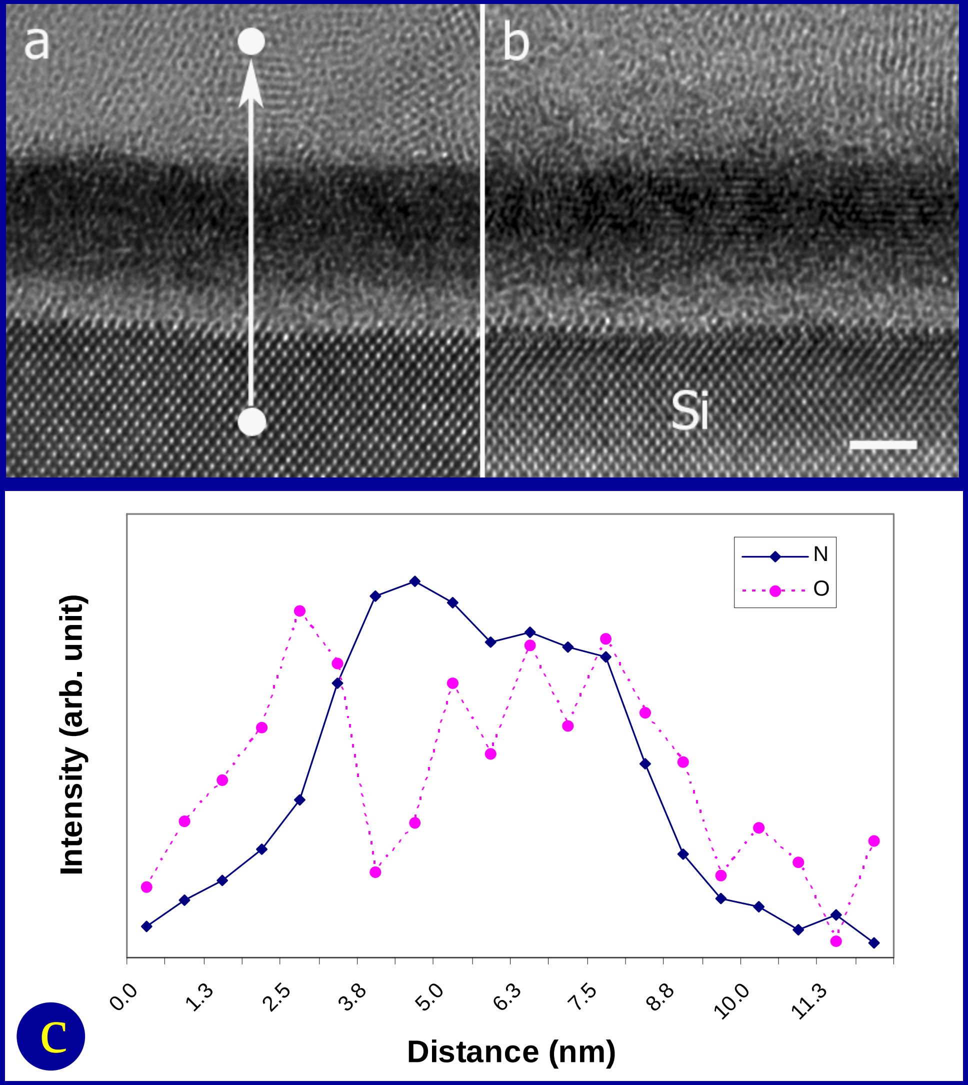

- Cross-sectional HRTEM images of the poly-Si capped thick $HfSi_xO_yN_z$ thin films on Si(100): (a) as-deposited, (b) 60 sec RTA at 1050ºC and (c) N and O concentration profiles across the interface shown in (a). The profiles are displaced vertically for easy comparison.
- Note nanocrystals and diffuse interfaces in the annealed.

HR(A)TEM: Application to Nano-X Materials

- Thermal stability of high-k gate dielectric films
  - Current SiO_2 gate oxide
  - ALCVD ZrO_2-based
  - $HfSiO_4$-based
  - $HfSi_xO_yN_z$-based

✓ Ultra low-k dielectric films
  - Nanoscale structural damage by plasma ash/etch
- Ni-silicides
  - Thin film morphology and phase identification
- Nanoscale lattice strain in Si CMOS Devices
  - New method of measuring local nanoscale strains

Ultra Low-K: Pore structure & Plasma damage

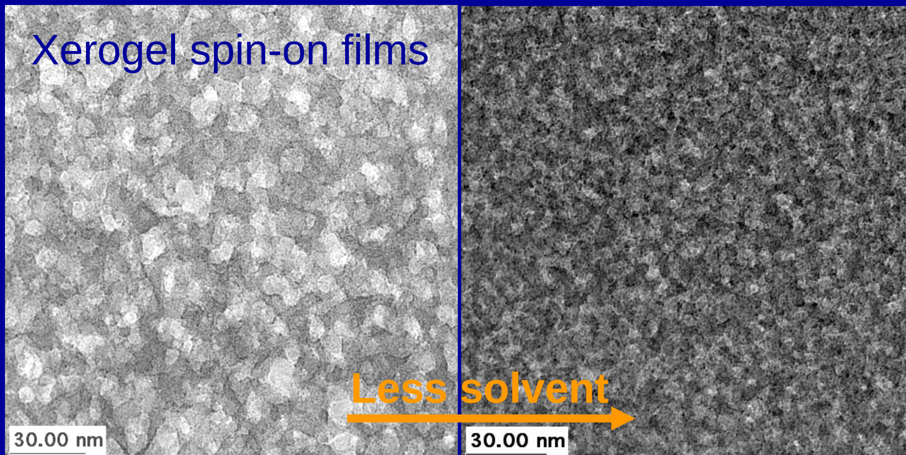

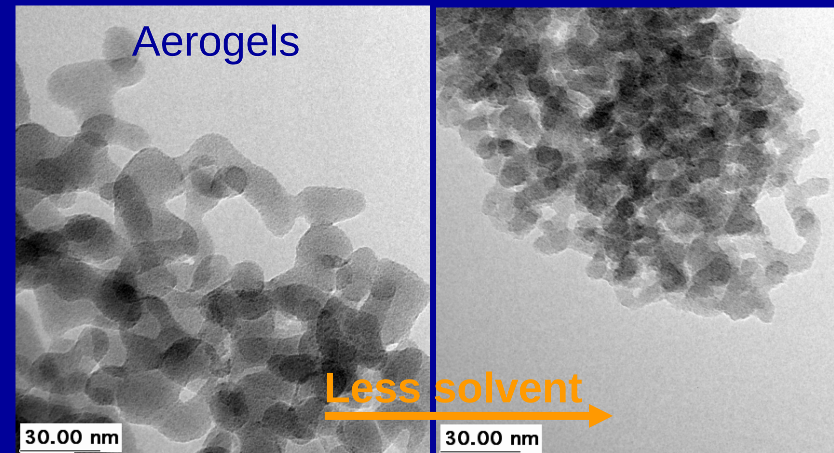

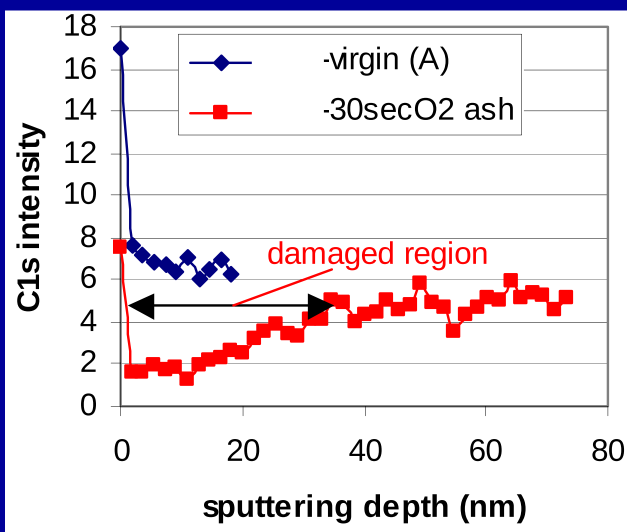

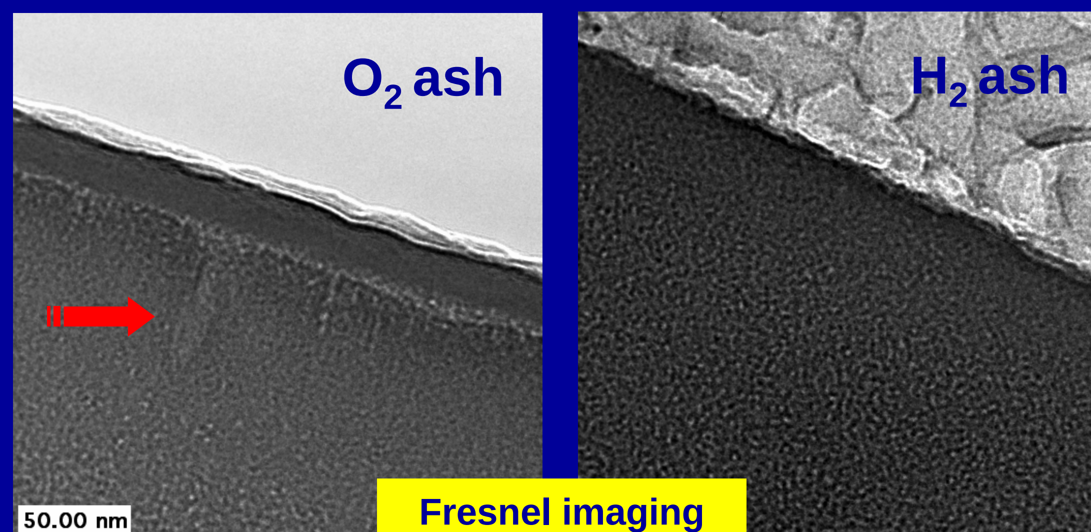

[Dong, Gorman, Zhang, Orozo-Teran, Roepsch, Mueller, Kim and Reidy, *J. Non-Cryst. Solids* **350**, 345 (2004)]

HR(A)TEM: Application to Nano-X Materials

- Thermal stability of high-k gate dielectric films
  - Current SiO_2 gate oxide
  - ALCVD ZrO_2-based
  - $HfSiO_4$-based
  - $HfSi_xO_yN_z$-based
- Ultra low-k dielectric films
  - Nanoscale structural damage by plasma ash/etch
- ✓ Ni-silicides
  - Thin film morphology and phase identification
- Nanoscale lattice strain in Si CMOS Devices
  - New method of measuring local nanoscale strains

UTD

Nano- Ni-Silicides

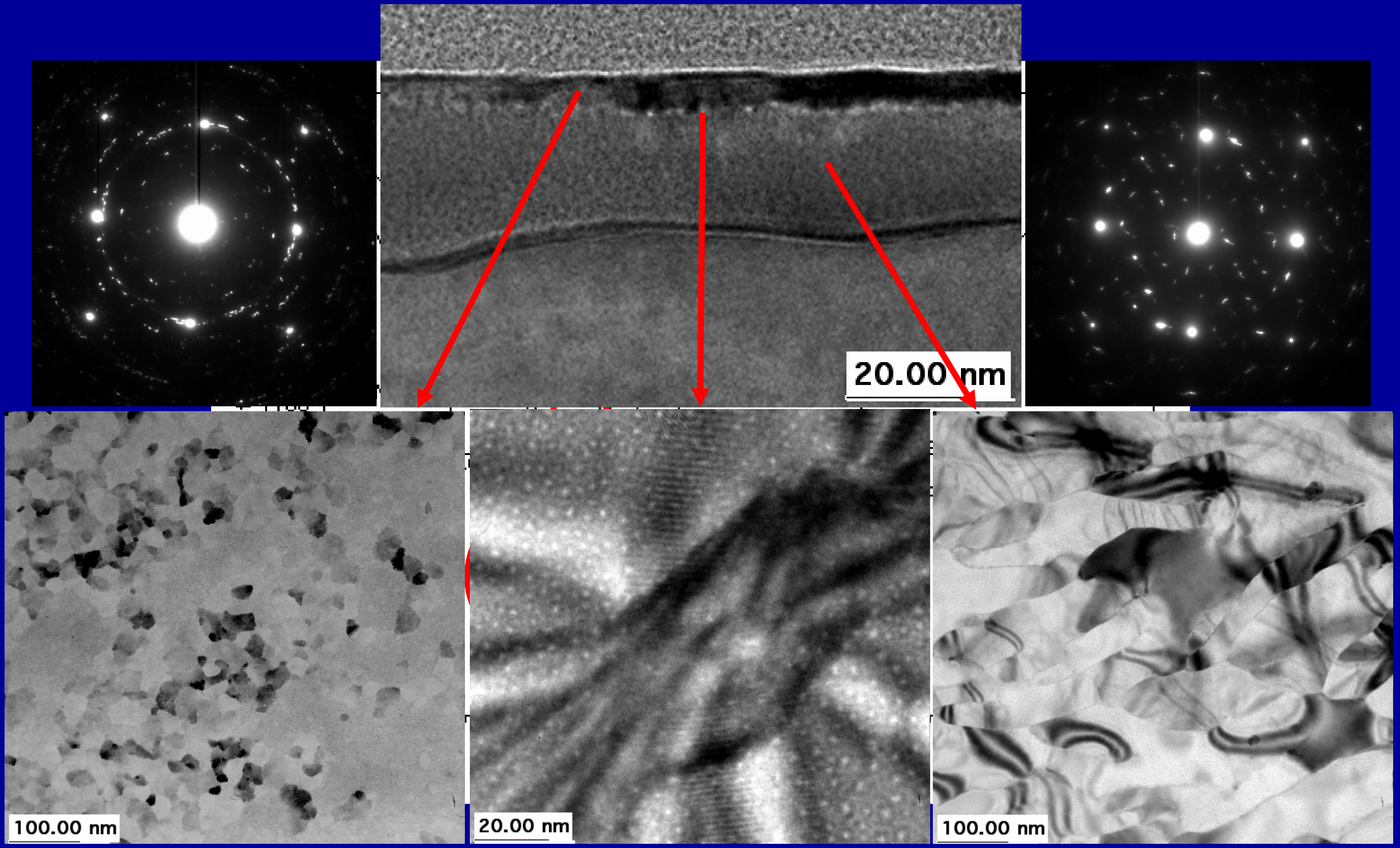

HR(A)TEM: Application to Nano-X Materials

- Thermal stability of high-k gate dielectric films
  - Current SiO_2 gate oxide
  - ALCVD ZrO_2-based
  - $HfSiO_4$-based
  - $HfSi_xO_yN_z$-based
- Ultra low-k dielectric films
  - Nanoscale structural damage by plasma ash/etch
- Ni-silicides
  - Thin film morphology and phase identification

✓ Nano-scale lattice strain in Si CMOS Devices
  - New method of measuring local nanoscale strains

Convergent Beam Electron Diffraction (CBED)

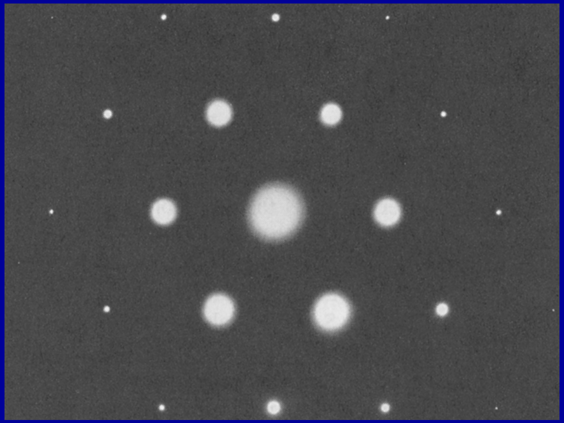

Selected Area Diffraction (SAD)

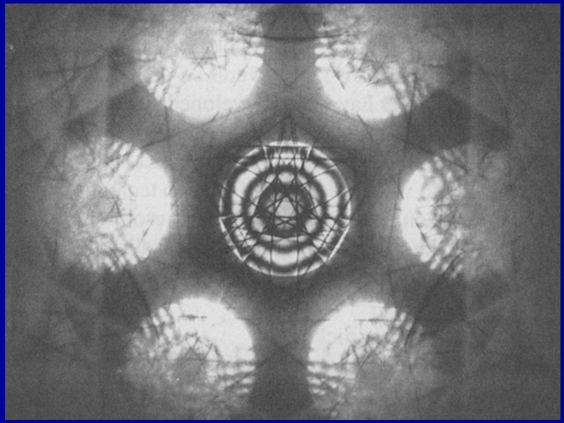

CBED

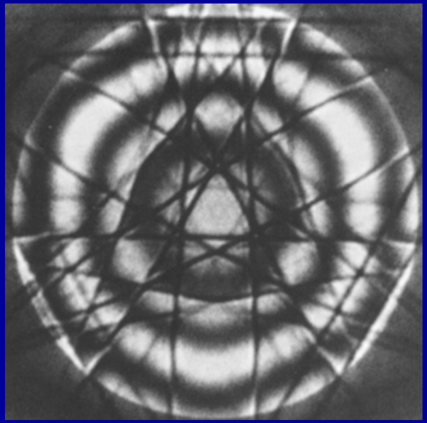

High Order Laue Zone (HOLZ)

- ✪ **Changes in the lattice parameter**
  → shifts in the HOLZ lines

$$\frac{\Delta\theta}{\theta} = \frac{\Delta a}{a}$$

- ✪ **Limit to the accuracy**

$$\frac{\Delta a}{a} = \frac{\Delta E}{2E} = \frac{40\ \text{eV}}{2 \bullet 100\ \text{keV}} = \frac{1}{5000}$$

- ✪ **Change of lattice parameter of an alloy or compound**
  → directly related to its chemical composition
  → deduced from shifts in the HOLZ line positions
- ✪ **Strains**
  → measured in an exactly equivalent fashion to the chemical changes
- ✪ **Spatial resolution**
  → depends on the probe size and its broadening by the specimen

MBE Grown Low Temperature InP

- ✪ Lattice parameter increase of ~0.09 nm ± 0.01nm (~0.15%)
  → excess phosphorus content of about 3% (Vegard's law)

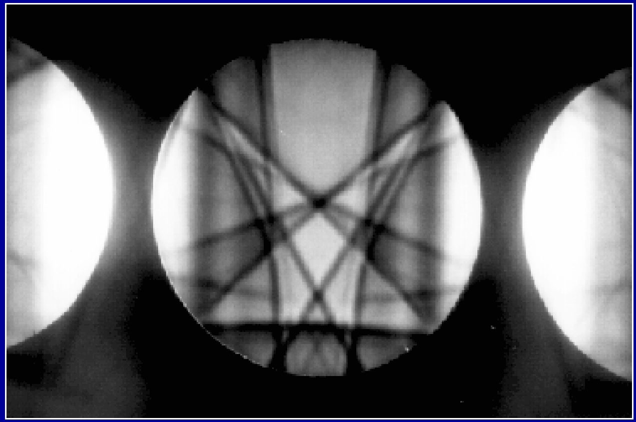

Experimental

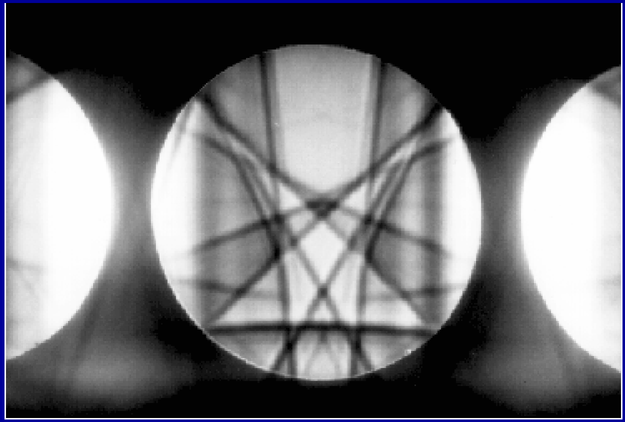

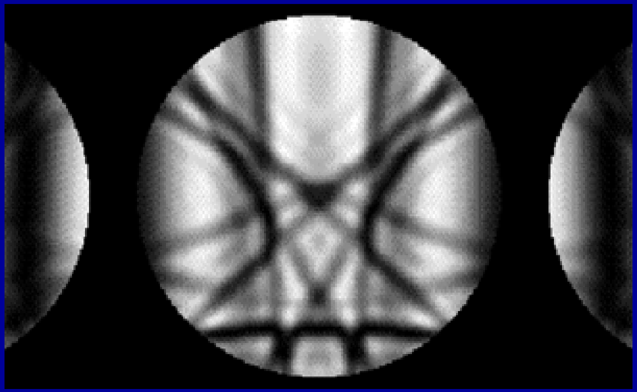

Simulation

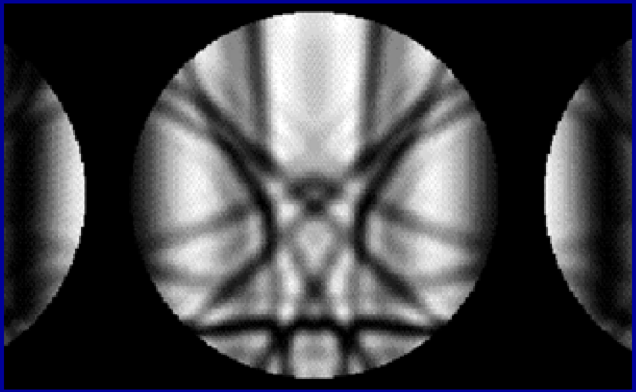

Top of the LT layer

Bottom of the LT layer

[Rajesh, Kim, Bow, Carpenter and Maracas, *Proc. 51st MSA*, pp. 810-811 (1993).]

True ('effective') Electron Beam Energy

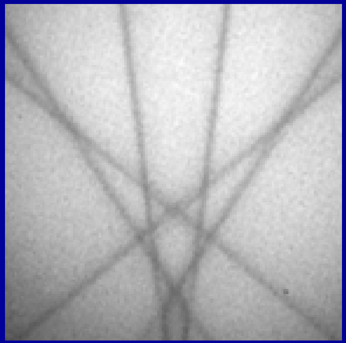

Silicon, unstrained, <230>, 200kV

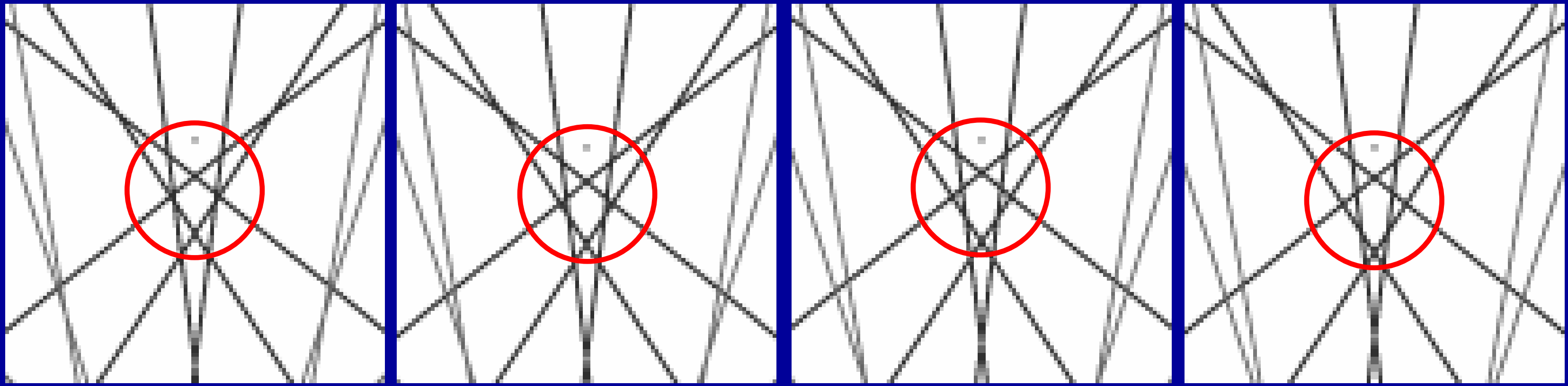

199.5 kV | 200 kV | 200.5 kV | 201 kV

- **Simulated HOLZ line patterns in the central CBED disc taken in the <230> zone axis based on the kinematical approximation, illustrating the effect of electron beam energy on the HOLZ line position.**

Effect of Strains

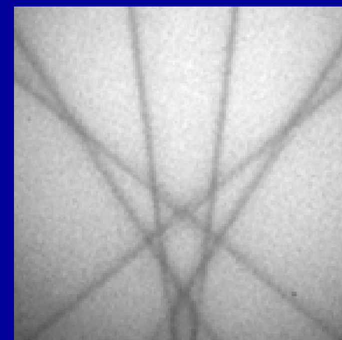

Silicon, <230>, 200kV

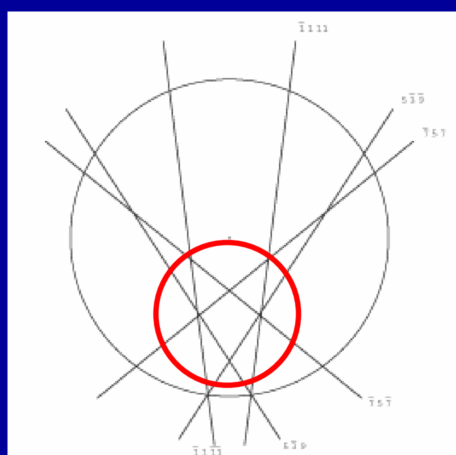

0.5415 nm

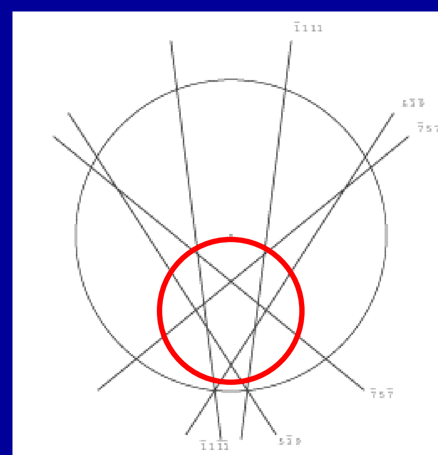

0.5431 nm

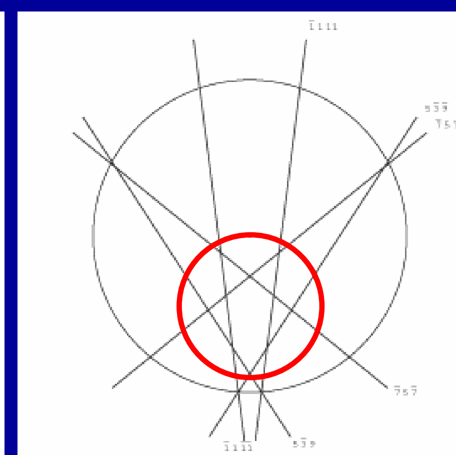

0.5447 nm

- **Simulated HOLZ line patterns in the central CBED disc taken in the <230> zone axis, showing the HOLZ line shifts due to changes in lattice parameter.**

Site-specific TEM Sample Preparation by FIB

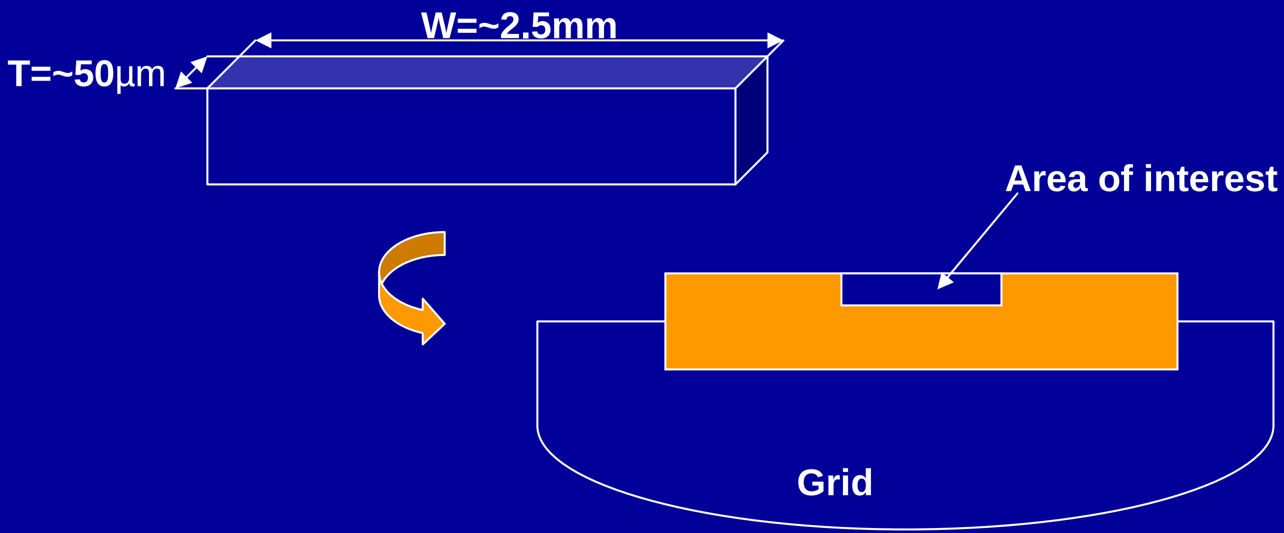

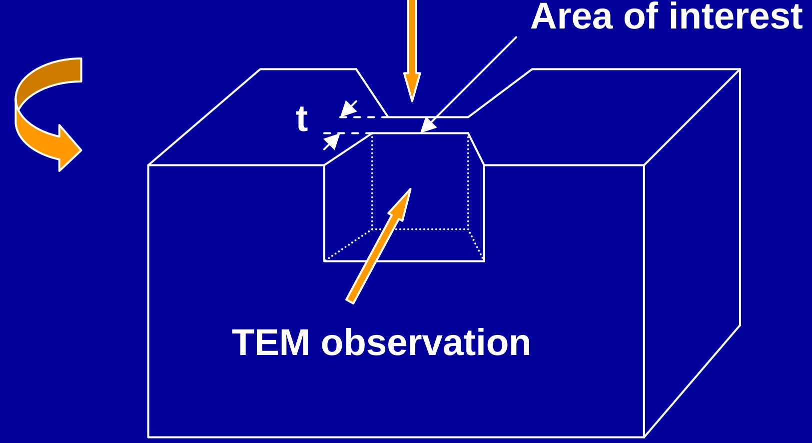

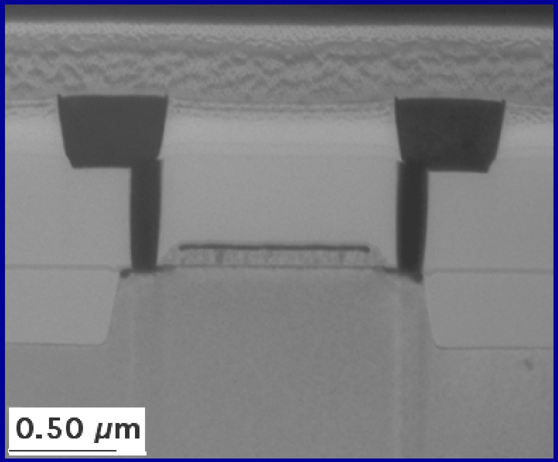

Nanoscale Strain in Advanced CMOS

- ✪ Local uni-axial strain approach with SiGe at the drain extension

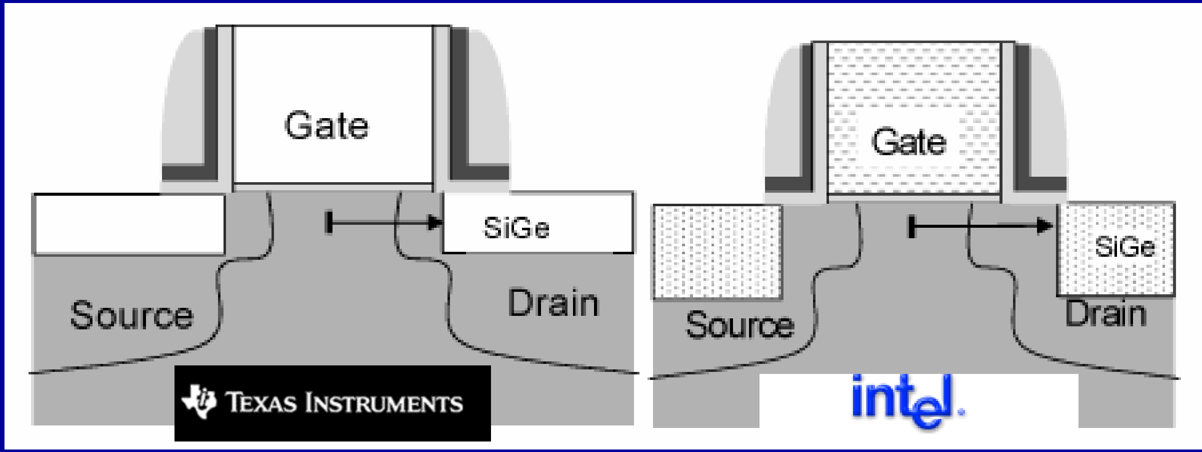

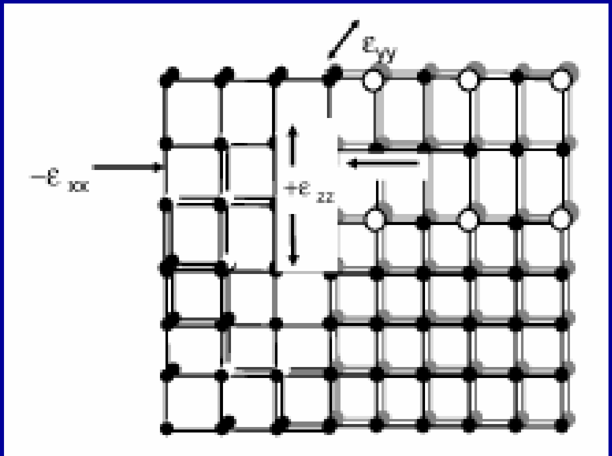

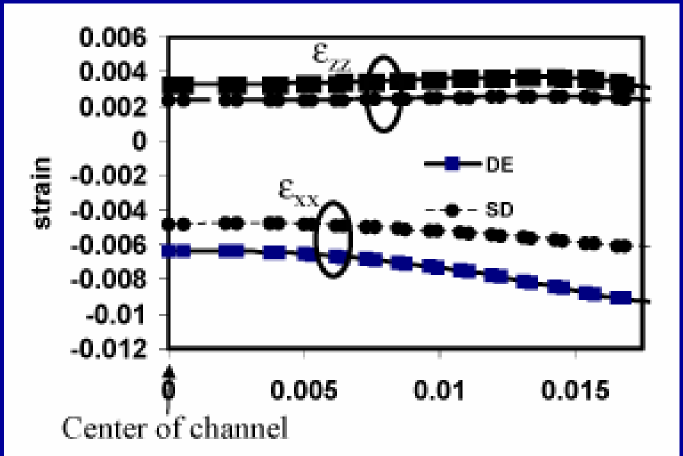

"***35% Drive Current Improvement from Recessed-SiGe Drain Extensions on 37 nm Gate Length PMOS***," P.R. Chidambaram, B.A. Smith, L.H. Hall, H. Bu, S. Chakravarthi, Y. Kim, A.V. Samoilov, A.T. Kim, P.J. Jones, R.B. Irwin, M.J. Kim, A.L.P. Rotondaro, C.F. Machala and D.T. Grider, VLSI 2004, 48-49 (2004).

Nanoscale Strain in Advanced CMOS

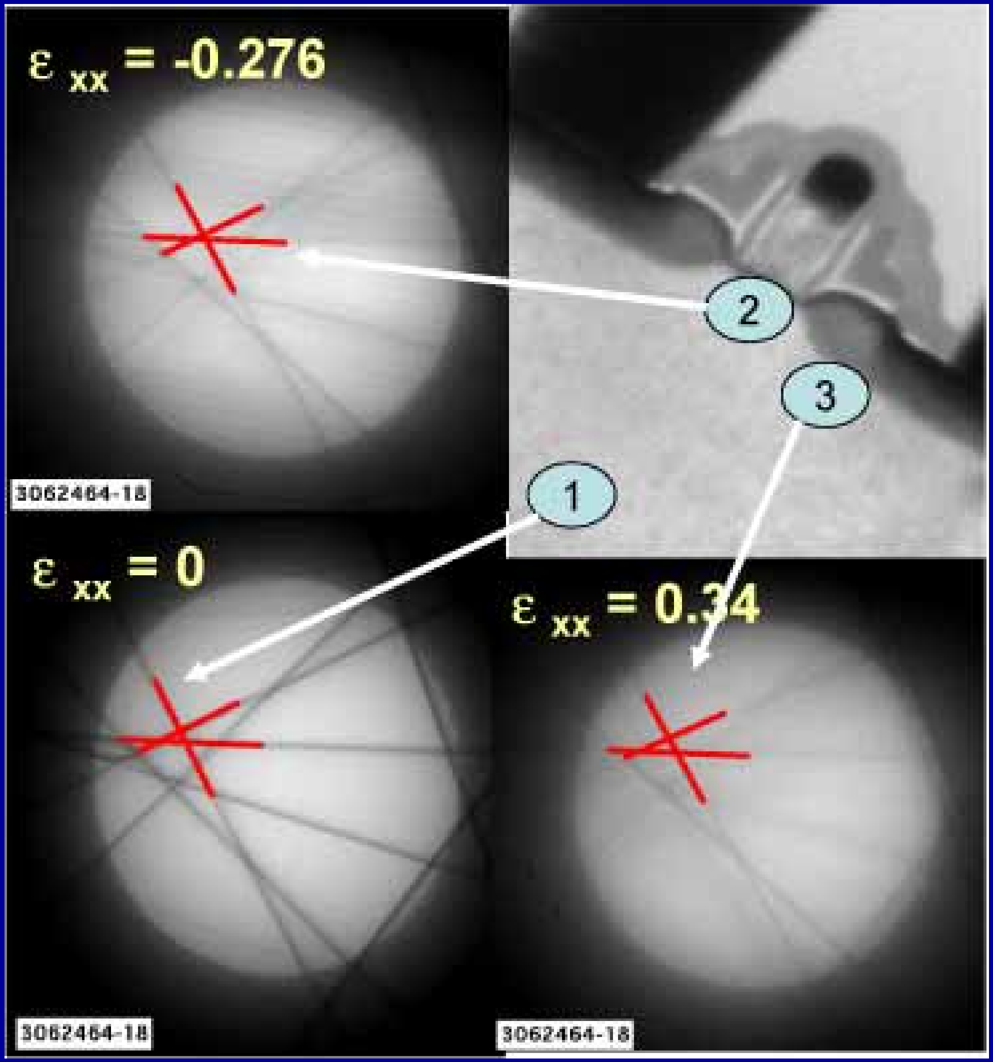

- Cross-sectional TEM image (left) of 37 nm gate with SiGe layer in the DE region.
- Convergent Electron Beam Diffraciton (CBED) patterns taken from the indicated area shown as insets. Lattice spacing measurements show ~0.3% peak compressive strain on silicon channel under the gate, and ~0.3% peak tensile strain below the drain.
- [“*Epitaxially strained SiGe process to improve mobility in the PMOS transistor*,” P. Chidambaram, B. Smith, L. Hall, H. Bu, S. Chakravarthi, Y. Kim, A. Samoilov, A. Kim, P. Jones, R. Irwin, M.J. Kim, C. Machala and D. Grider, *ECS Proc*. **2004-07**, 123-134 (2004).]

Energy-filtering

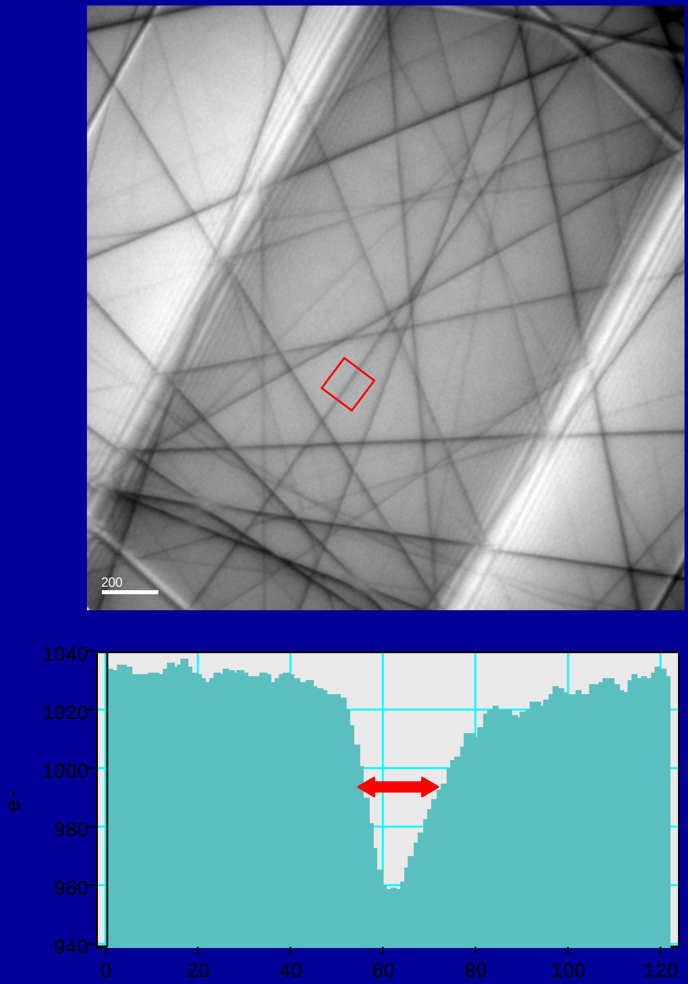

Unfiltered

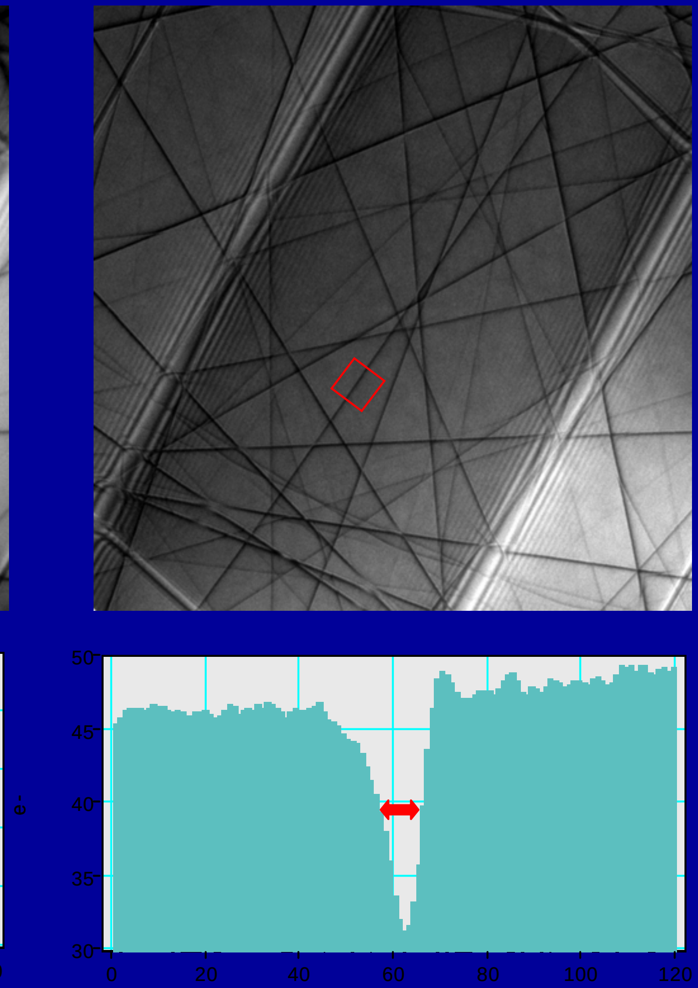

RT energy-filtered

Nanoscale Strain in Advanced CMOS

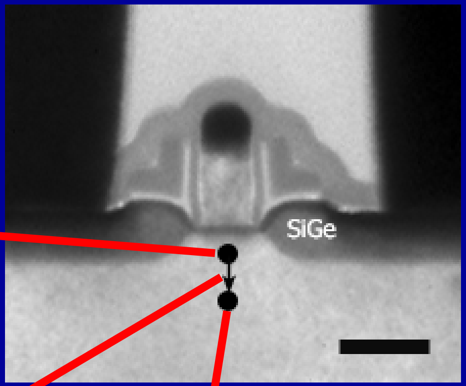

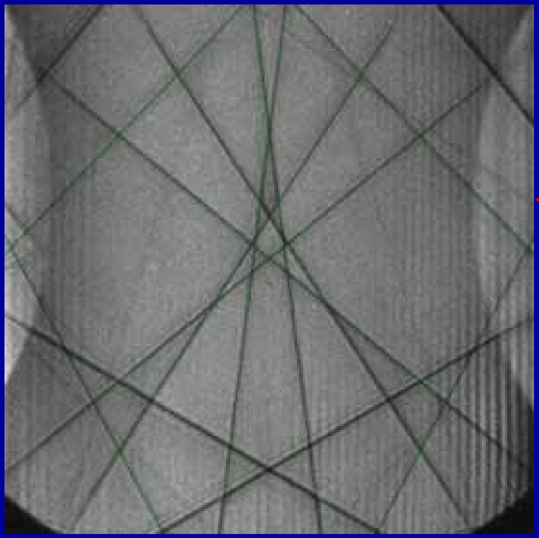

-0.276%

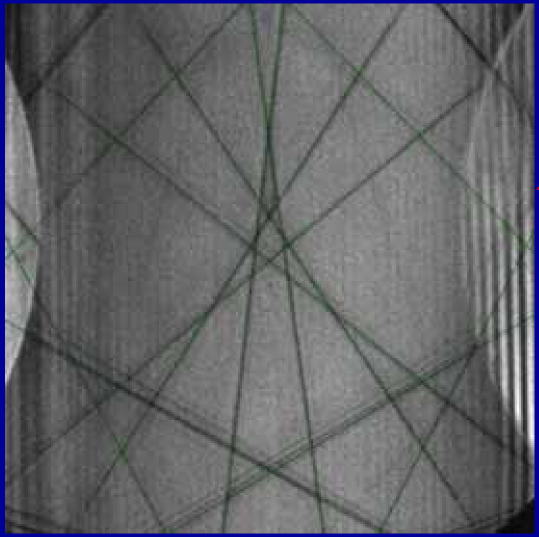

-0.203%

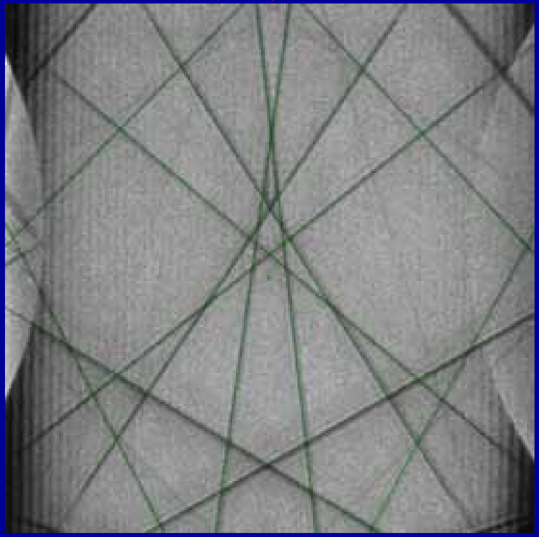

-0.129%

Experimental <230> CBED patterns, superimposed by the simulated ones, showing a compressive strain gradient that decays from the center channel region.

Nanoscale Strain in Advanced CMOS

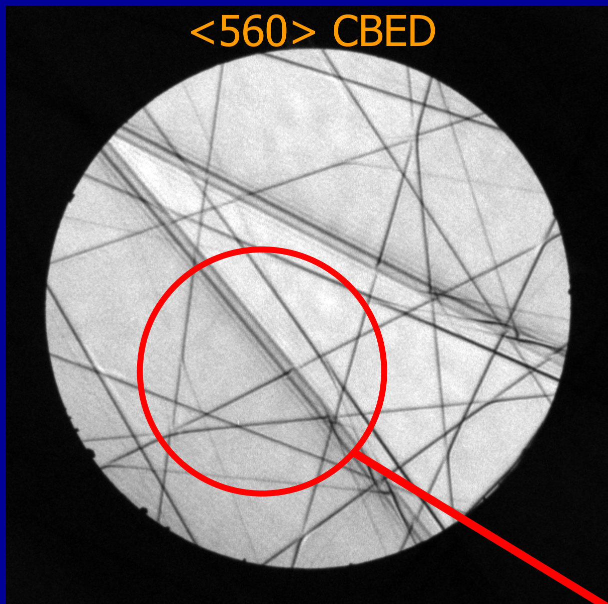

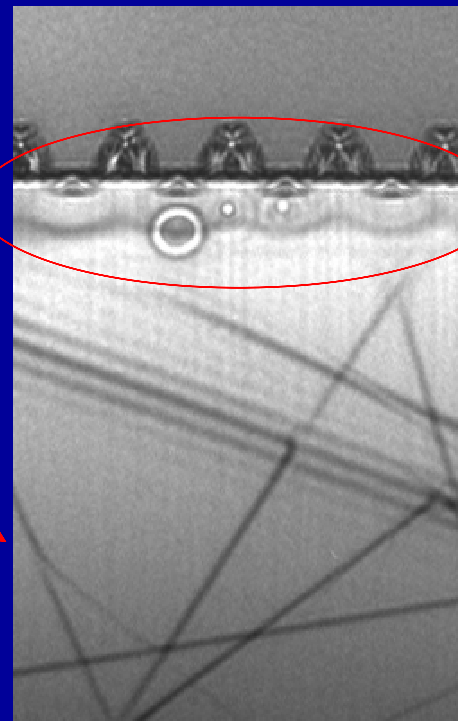

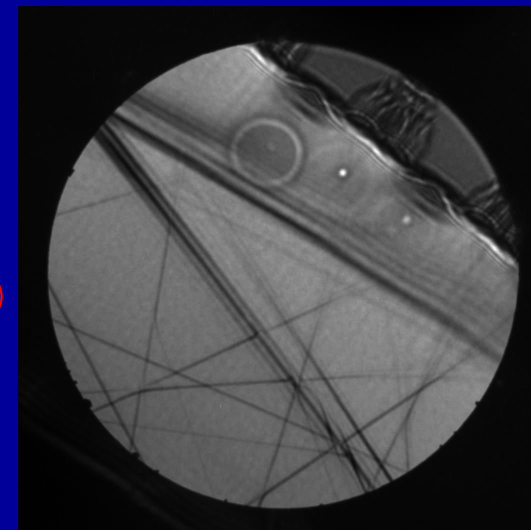

<560> convergent beam shadow images.

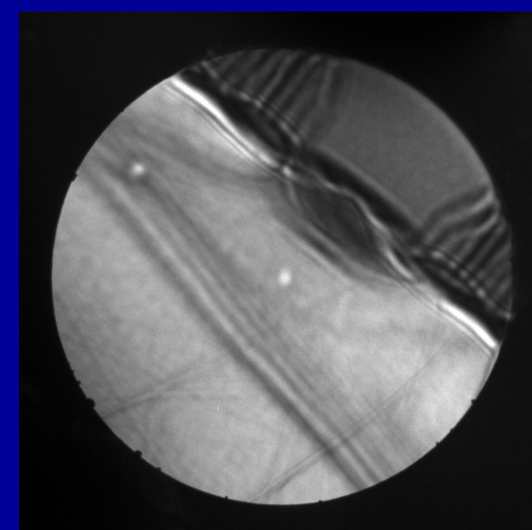

Conclusions

- ✪ Resolution limits
  - Aberration-corrected TEM/STEM
    - → < 0.1 nm spatial resolution
    - → < 0.1 eV energy resolution
  - Practical
    - → Radiation effects
      - ❖ Mass loss
      - ❖ Displacement damage
    - → Quality of TEM samples
      - ❖ Preparation methods
      - ❖ Contamination, Preferential milling
    - → Probe/Specimen stability
      - ❖ Environment
- ✪ Future
  - Remote operation, in-situ
  - Nano and Beyond ⇪

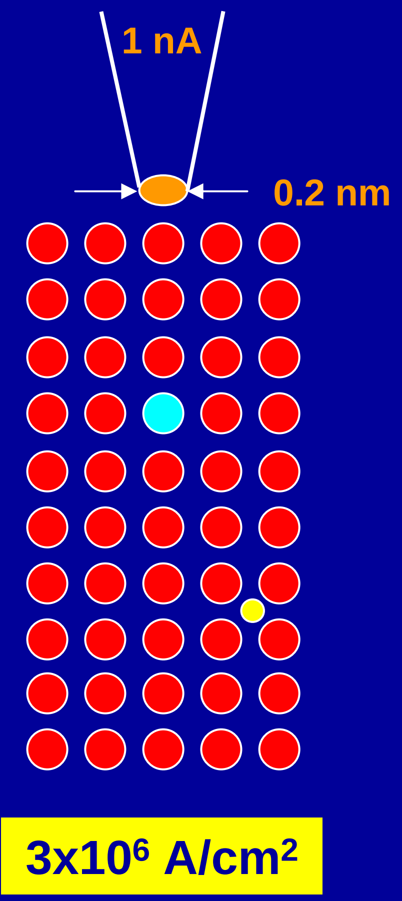

Acknowledgements

<u>Collaborators</u>

R.W. Carpenter
P.R. Chidambaram
M. Quevedo-Lopez
J. Kim
H. Edwards
R. Irwin
P. Jones
E. Koontz

<u>Students</u>

J. Huang
D.K. Cha
J.B. Jeon
T.H. Lee
P. Zhao
P. Sivasubramani

VNB Modification in TEM

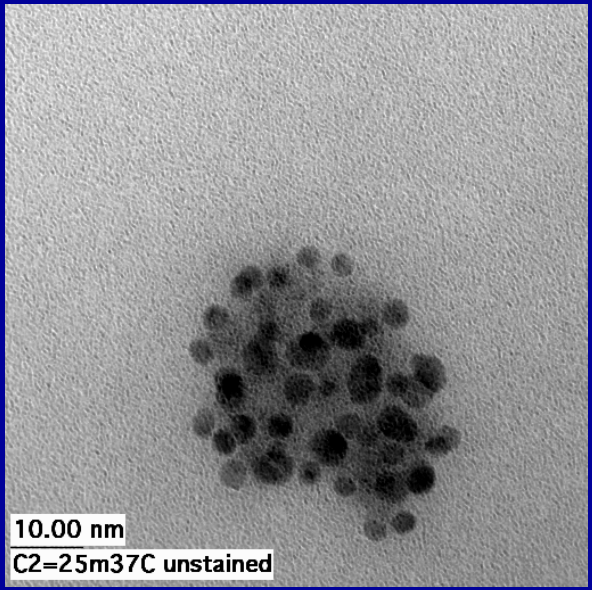

As-received, unstained VNB with 5 nm Au particles attached

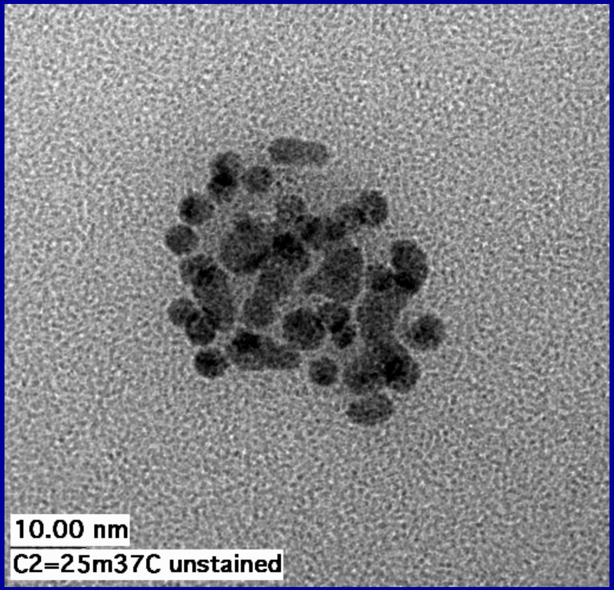

After 2 min e-beam exposure.
Note contact between Au particles

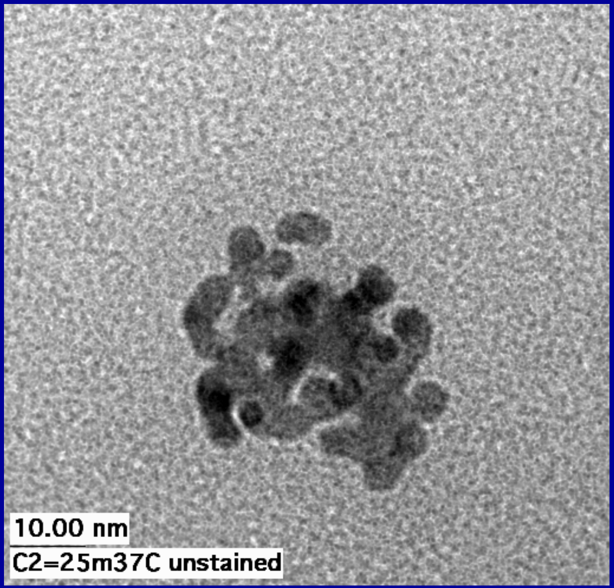

After 4 min e-beam exposure, increased Au "melting"

Direct Wafer Bonded Ge/Si

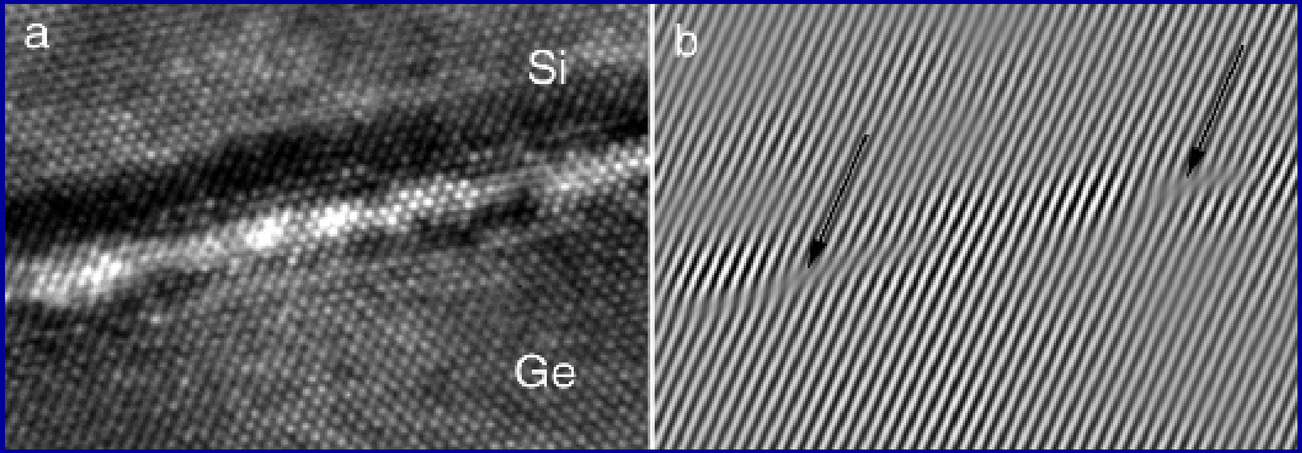

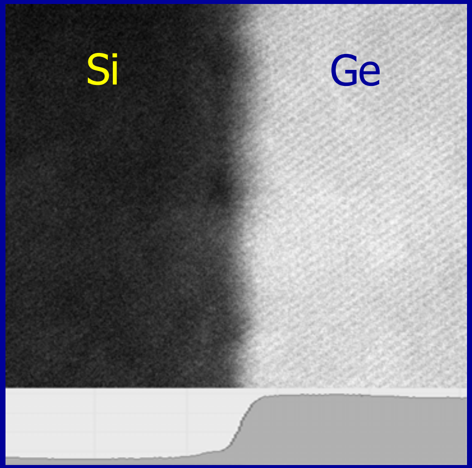

- HREM (a) image of the bonded Ge/Si interface. Their 4% lattice mismatch accommodated by misfit dislocations along the interface (b). (Left) Z-contrast image shows the chemical width of the interface to be about 2 monolayers. (Right) Low voltage I-V curve of the bonded p-Si/n-Ge heterojunction.